nature geoscience

Article

https://doi.org/10.1038/s41561-025-01742-z

Limited carbon sequestration potential from global ecosystem restoration

Received: 3 March 2024

Accepted: 10 June 2025

Published online: 31 July 2025

Check for updates

Csaba Tölgyesi[1,2,14] ✉, Nándor Csikós[1,3,14], Vicky M. Temperton[4], Elise Buisson[5], Fernando A. O. Silveira[6], Caroline E. R. Lehmann[7,8], Péter Török[2,9,10], Zoltán Bátori[1,11] & Ákos Bede-Fazekas[12,13]

Ecosystem restoration is increasingly recognized as a means of climate change mitigation. Recent global-scale studies have suggested that ecosystem restoration could offset a substantial fraction of human carbon emissions since the Industrial Revolution. However, global carbon sequestration potential remains uncertain due to the tree-centric view of some models and difficulties in modelling restoration across different ecosystem types. Here we applied a model-based prediction workflow to estimate the carbon capture potential of restoring forest, shrubland, grassland and wetland ecosystems until 2100. We found that the maximum sequestration potential is 96.9 Gt of carbon, equivalent to 17.6% of the anthropogenic emissions to date, or 3.7–12.0% if taking into account future emissions until 2100. Our results suggest that ecosystem restoration has limited potential for climate change mitigation even if orchestrated with a pervasive shift towards sustainable, low-emissions economies globally. In addition, if we plan restoration targets to match future climatic conditions and consider state transitions of currently natural ecosystems due to climate change, the potential for natural climate solutions related to ecosystem restoration is close to zero. Therefore, we recommend that ecosystem restoration is pursued primarily for restoring biodiversity, supporting livelihoods and resilience of ecosystem services, as the climate mitigation potential will vary depending on the state transitions that occur between vegetation types.

In 2024, the European Parliament passed the ambitious Nature Restoration Law to address the biodiversity crisis by initiating ecosystem restoration in 20% of the European Union's land and maritime areas until 2030 and in all degraded habitats of member states by 2050[1]. The EU initiative aligns with global movements, including the UN Decade on Ecosystem Restoration, launched to halt biodiversity loss and secure human well-being on a long-term basis[2,3]. Most biodiversity initiatives are linked to the mitigation of anthropogenic climate change through ecosystem-scale carbon storage. The EU Nature Restoration Law explicitly states that accelerating and up-scaling ecosystem restoration will contribute to climate change mitigation.

There is wide consensus that reducing greenhouse gas emissions is central to climate change mitigation[4], but recapturing atmospheric CO_2 is also necessary to reach climate targets[5–7]. Technological solutions for atmospheric CO_2 removal are today unavailable at relevant scales[8]. Conversely, natural climate solutions (NCSs) are considered straightforward and rely, among others, on the ability of plants to capture CO_2 and store carbon in their tissues or later in the soil.

Ecosystem restoration includes revegetation of degraded land to a reference state, thus qualifying as an important NCS via capturing CO_2. However, the potential of ecosystem restoration to offset anthropogenic emissions remains controversial. Given the urgency

A full list of affiliations appears at the end of the paper. ✉e-mail: festuca7@yahoo.com

to act and the opportunity to up-scale ecosystem restoration from the mid-2020s, a clear picture of the realistic impact of ecosystem restoration is required.

Influential studies provided promising model outputs[9,10], suggesting up to two-thirds of the anthropogenic carbon burden can be recaptured with restoration-based NCS. However, Bastin et al.[9] received criticism for their tree-centric view of global ecosystems that ignored diverse ecosystem types and overlooked negative afforestation impacts on biodiversity and ecosystem functioning of non-forest ecosystems[11–13]. Open ecosystems (for example, grasslands and savannahs) with their unique biodiversity and ecosystem services, also sequester considerable amounts of carbon[14]. Unlike in forests, open ecosystem carbon stores are mostly belowground, out of reach from fire and drought, processes to which these ecosystems have a high resilience, and that in forests substantively reduce aboveground carbon[15–17]. Into the future, open ecosystems may be a more secure land-cover type to store carbon in fire-prone regions[15]. Empirical studies have shown that fire-suppression-driven increases in tree cover of historically open ecosystems has limited impact on total ecosystem carbon stocks[18]. Furthermore, open ecosystem afforestation increases water scarcity[19,20], alters fire regimes, reduces biodiversity[21] and albedo, which can offset or outweigh climate benefits[22,23].

Strassburg et al.[10] addressed some of the above issues by modelling the potential carbon gain of restoring a range of ecosystems and found values similar to Bastin et al.[9]. However, they used a method to predict potential ecosystem types earmarked for restoration that generates high uncertainty. Examining the current composition of every 4.96 × 4.96 km pixel on Earth's terrestrial surface, they identified natural-looking ecosystem patches and used the proportion of each to extrapolate to the entire pixel, an approach appropriate for homogeneous landscapes but yields high uncertainty in mosaic landscapes (for example, open-forest mosaic, topographically or hydrologically complex landscapes)[24–26] where uniform anthropogenic impacts were highly unlikely. Furthermore, partially degraded areas are largely overlooked[27], and woody vegetation, including non-native plantations, were considered natural looking. Therefore, non-forested landscapes converted to arable land with some planted trees were considered potential forest restoration areas. This bias led, for example, to predicting forest restoration across the Carpathian Basin in Eastern-Central Europe, home to the largest stretch of intact steppe grassland within the European Union. Moreover, Bastin et al.[9], Strassburg et al.[10] and a recent tree-centric model by Mo et al.[28] considered total carbon stocks, although reaching those values by 2100 seems unlikely in certain ecosystem types, especially if restoration is not performed instantaneously but with a realistic schedule over the twenty-first century.

At the low end of the predicted carbon sequestration potential, Cook-Patton et al.[5] listed ecosystem restoration as the least effective of the main NCSs, with protecting intact ecosystems and improving land management ranked as best alternatives. This aligns with Mo et al.[28], who also focused on increasing carbon stocks of existing forests. Nolan et al.[6] then highlighted the uncertainty of restoration-mediated CO_2 removal, given the tenfold difference between current highest and lowest predictions. The low predicted values of some models are due to potential difficulties in realizing large-scale ecosystem restoration due to social, economic and governance constraints. Recently, some of these constraints have started to be alleviated via top-down mechanisms such as the EU Nature Restoration Law. Williams et al.[29] provide a partial solution for economic and governance constraints via effective ongoing unassisted large-scale forest regeneration, requiring minimal intervention but potentially contributing >2.15 million km^2 of forest gain within 30 years.

Relying on previous modelling approaches and via addressing the criticisms they received, we present results of a global ecosystem restoration model. In our approach (Fig. 1), we applied machine learning to predict the potential cover percentages of native ecosystem types to terrestrial locations using climatic, soil and topographic predictors (Extended Data Table 1). We then assessed the potential restorable area for each ecosystem. Using published carbon sequestration rates for each ecosystem type, we calculated expected global carbon gain until 2100. Our estimates may be more realistic than previous ones because we account for (1) all major terrestrial ecosystem types, (2) above- and belowground carbon storage, where relevant, (3) carbon sequestration rates (instead of total stocks, which often require > 70 years, that is the length of the 2030–2100 planning period, to develop), (4) the carbon sequestration rate of current ecosystem type (because the net carbon gain is the difference between current and post-restoration rates), (5) biogeographic differences, (6) socio-economic considerations that exclude built-up and intensive agricultural areas from restoration and (7) sustainable land-use practices in restoration targets (that is, certain high-nature-value farming landscapes, such as wood pastures, can also be predicted as targets), (8) future carbon emissions, (9) a schedule of restoration implementation and (10) current and future (2061–2080) climatic conditions to predict restoration targets. Using our model, we estimate how global ecosystem restoration can potentially contribute to climate change mitigation until 2100.

Available areas for restoration

Using current climate, we predicted a total of 42.48 million km^2 of forest, 14.14 million km^2 of shrubland, 36.07 million km^2 of grassland and 3.10 million km^2 of wetland on Earth's land surface as potential natural ecosystems (Fig. 2a–d). The majority has been greatly altered by human actions[30], but according to our model, 28.76 million km^2 are available for ecosystem restoration. Of this, 11.66 million km^2 (40.5% of the total area) is potential forest (Fig. 2e), slightly higher than the 9 million km^2 predicted by Bastin et al.[9], but lower than the 15.50 million km^2 of Strassburg et al.[10]. We found large potential areas for forest restoration (including restoring the forested component of mosaic landscapes) across the northern temperate and boreal zones and across subtropical and tropical regions. Nearly 4.91 million km^2 (17.1%) was suitable for shrubland worldwide as the target of ecosystem restoration (Fig. 2f), particularly in eastern Australia and southern-central United States, a figure similar to the Strassburg et al.[10] prediction (4.11 million km^2).

The total area for grassland restoration is 9.37 million km^2 (32.6%), ~30% higher than Strassburg et al.'s[10] 7.17 million km^2, implying overestimation of forest expansion at the expense of grassland. Potential grassland restoration in our model is concentrated in North America, Eurasia, Asian highlands and tropical mosaics (Fig. 2g). Large potential grassland restoration targets were predicted at the northern edge of boreal forests, potentially indicating misplaced tree plantations or other forms of degradation due to grassland overuse or a lagging of climate-change-driven expansion of grassland on currently sparsely vegetated areas.

Total area predicted for wetland restoration including all freshwater and saltwater herbaceous wetlands (excluding permanent water and wooded wetlands) was 2.83 million km^2 (9.8%), concentrated in the American Midwest and Eastern Asia, where wetlands have been extensively drained for agriculture[31,32]. Potential wetland restoration was also identified in many floodplains and coastal habitats, such as the Euphrates River and Gulf of Bengal (Fig. 2h). Strassburg et al.[10] calculated potential wetland restoration at 0.57 million km^2, and they were explicit wetland restoration was probably underestimated. However, our model's predictive power was also comparatively low for wetlands.

Using a climate scenario projected for 2061–2080 (that is, the middle of our planning period) may potentially provide more relevant target ecosystems as in the future, sites may become available for restoration if a current native ecosystem type will no longer be a potential predicted ecosystem type. These state transitions may happen spontaneously (for example, tree encroachment in present-day tundra or grassland expansion due to excessive fires in dry tropical forests) but can also be actively assisted if the transition is for some reason favourable.

https://doi.org/10.1038/s41561-025-01742-z

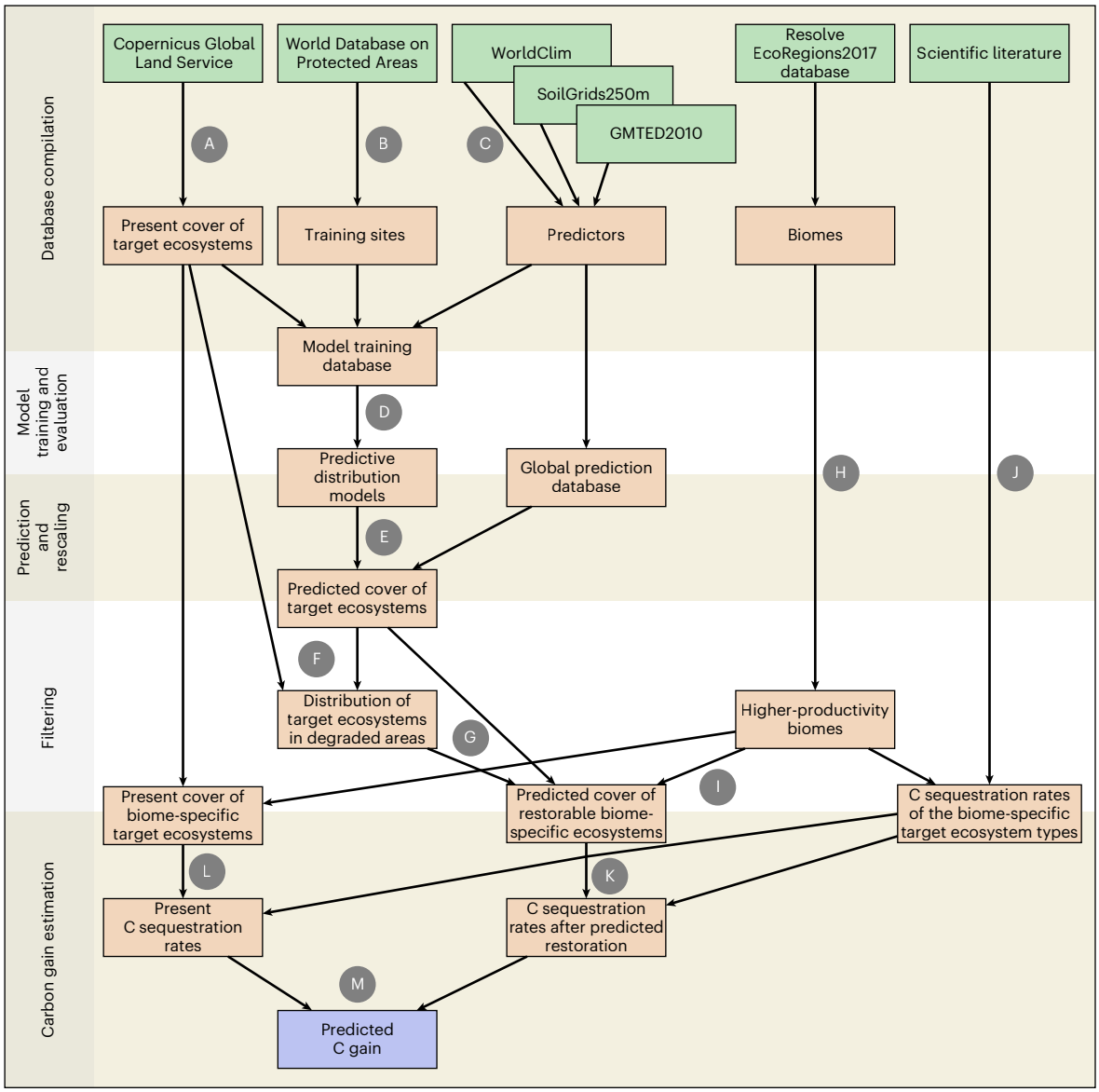

Fig. 1 | Flowchart of the modelling process to predict the carbon gain potential of global ecosystem restoration until 2100. Detailed description of the steps marked with capital letters A to M can be found in Methods. Extended Data Figs. 6–8 provide further details of the model. Boxes in green are external sources of input data, orange boxes signify intermittent datasets and models and the blue box is the final output. Horizontal tan shading separates the main steps of modelling and prediction.

Predicted 2061–2080 potential forest extent is 35.9–37.4 million km^2, depending on the climate scenario (SSP1–2.6, SSP2–4.5, SSP3–7.0 or SSP5–8.5), with forest expansion at high latitudes but widespread loss in tropical zones (Extended Data Figs. 1–4a). The latter is especially prevalent in the Amazon Basin, as forecast by other studies[33–35]. Taking such modelled state transitions into account includes both expansion and loss compared to the present, with a net outcome that is negative, indicating 2.3–3.4 million km^2 forest loss globally (Extended Data Figs. 1–4e).

Compared to current predictions, future potential shrubland area doubles, mostly due to potential forest loss, and reaches 11.2–11.7 million km^2 (Extended Data Figs. 1–4b) with a net available amount for restoration and state transitions of 0.7–1.1 million km^2 (Extended Data Figs. 1–4f). Grasslands (and savannahs) expand their potential area, predicted to increase to 26.9–28.8 million km^2, largely due to savannah expansion, montane grassland cover growth in Tibet and forest-steppe expansion over boreal forests (Extended Data Figs. 1–4c). However, dependent upon the combination of climate scenario, restoration opportunities and state transitions, there is a combined change from a loss of 0.6 million km^2 to a gain of 1.1 million km^2 (Extended Data Figs. 1–4g). Conversely, potential future wetland area, amounting to 3.7–5.2 million km^2 (Extended Data Figs. 1–4d), is not only higher than current potential, but 2.6–3.8 million km^2 will be available for restoration and state transitions (Extended Data Figs. 1–4h).

Carbon capture potential

Overall, restoration of available land (all potential land minus areas with natural vegetation, built-up and intensive agricultural areas and arid and polar regions) using current climate predictions would lead to carbon capture of 1.92 Gt yr^{-1}, summing to a total of 136.3 Gt between 2030 and 2100 (Fig. 3). However, reclaiming all this land by 2030 and initiating target ecosystem restoration are extremely unlikely. Using the momentum of the UN Decade on Ecosystem Restoration combined with the targets of the EU's Nature Restoration Law, feasibility

https://doi.org/10.1038/s41561-025-01742-z

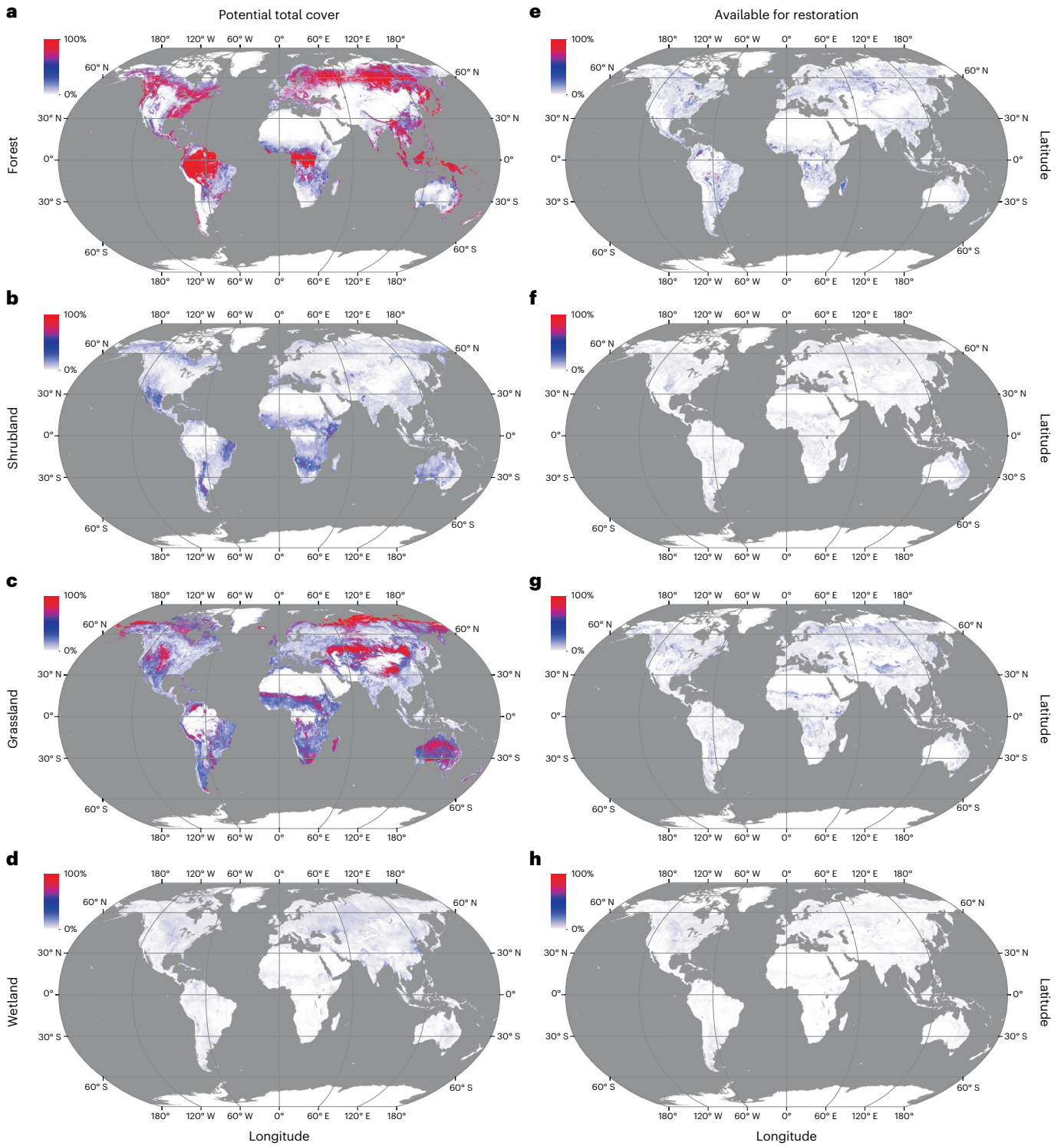

Fig. 2 | Potential distribution of modelled ecosystems and the available area for restoration using current climates for predictions. a–d, Potential distribution of modelled forest (**a**), shrubland (**b**), grassland (**c**) and wetland (**d**) ecosystems using current climates for predictions. **e–h**, The available area for forest (**e**), shrubland (**f**), grassland (**g**) and wetland (**h**) restoration. Colour coding indicates the percentage of each ecosystem type (predicted and restorable) within a 1 × 1 km grid. Thus, ecosystem combinations (for example, forest steppes and savannah-forest mosaics) are also allowed in our grid-level restoration planning, although the proportion of each constituting ecosystem type appears on different maps. For example, a savannah-forest mosaic landscape can contain forested, shrubby and grassy parts within a grid cell, and their proportional values are shown on each of the three corresponding maps. Available area is the potential area minus (1) intact areas not requiring restoration, (2) intensive agricultural areas, (3) built-up areas and (4) biomes with low productivity (polar and arid regions).

calculations[36] and the potential of natural regeneration[29], achieving 20% of the potential area is theoretically possible for restoration initiation by 2030. The remaining 80% could be implemented evenly across the 2031–2100 period (Fig. 4). This more realistic timeframe suggests sequestration of 85.2 Gt by 2100. Of this, 49.4 Gt (58.1%) is allocated to forests, which is substantially less than either Bastin et al.[1] or Mo et al.[28]. Open ecosystems combined sum to 35.8 Gt (41.9%). Including the three main open ecosystems in global agendas can thus

https://doi.org/10.1038/s41561-025-01742-z

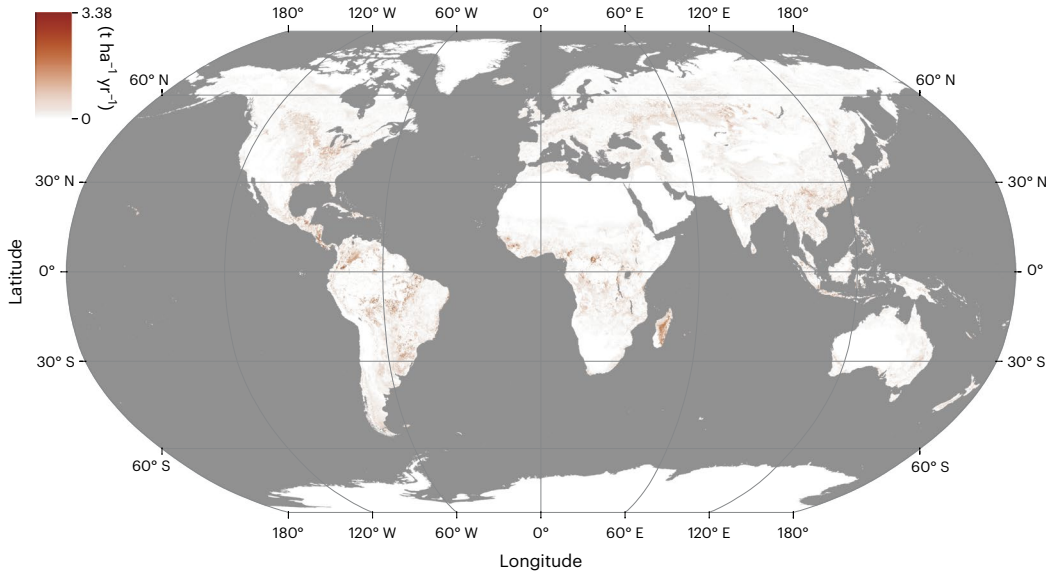

Fig. 3 | Global distribution of potential annual carbon gain rates of all restorable land predicted using current climates. A global maximum sequestration rate gain of 1.92 Gt yr^{-1} can be achieved using restoration, of which 67.4%, 9.2%, 12.3% and 11.4% come from restored forests, shrublands, grasslands and wetlands, respectively. Carbon gain includes both above- and belowground carbon capture (except in savannah grasslands where we considered only belowground rates due to frequent fires). Shown carbon gain rates are calculated as the difference between the rates of the predicted restoration targets minus the rates of the current ecosystem types in 1 × 1 km modelling sites. We used biome-specific rates for each of the four ecosystem types instead of global averages.

nearly double potential carbon sequestration, while also provide a control on misplaced tree planting and afforestation with undesired effects, such as warming due to reduced albedo[22,23,37], increased wildfires[15] and biodiversity declines.

The above 85.2 Gt can be increased by prioritizing regions with the highest potential carbon benefit. For this, we laid a grid of 100 km × 100 km mesh size on the terrestrial surface of Earth and selected those cells as priority regions that cover 20% of the potentially restorable area with the highest possible carbon gain. Starting restoration until 2030 within these priority regions and then continuing randomly with the rest increases capture to 96.9 Gt carbon until 2100. These priority regions include temperate areas, such as American prairies and central Asian steppes (Fig. 4), and not only formerly prioritized tropical rainforest regions[29]. On reflection, we probably received this nuanced pattern over previous studies via our ecosystem-inclusive approach, the use of rates over final carbon stocks and that we did not ignore the carbon sequestration of the ecosystem type before restoration. As a result, there is a more even biogeographic distribution of priority regions, with greater opportunities for both high- and low-income countries to contribute to large-scale restoration, supporting climate justice, ameliorating an increasing pressure on historically low-emitting countries to meet ambitious restoration targets[29,38,39]. The inclusion of non-forested ecosystems offers the promise of more equitable global NCS efforts than, for example, simplistic tree-planting campaigns. Such campaigns driven by carbon credits may eventually have little climate change mitigation[37,40,41] and rather have detrimental impacts on biodiversity[21] and livelihoods of local people[42–44], for example, by displacing people for afforestation, which in turn can lead to deforestation elsewhere. In addition, future agricultural expansion in low-income countries can cause conflicts with the realization of ecosystem restoration predicted on the scale of the present study. The total area allocated to agriculture is expected to be more stable in high-income countries[45], making them also perhaps sustainable targets of restoration interventions.

Our estimate of 96.9 Gt carbon sequestration potential is substantially smaller than previous models[9,10], as it equals to 47.3% and 31.8% of their respective predictions, and amounts to 17.6% of the 640 Gt of carbon emissions since 1750[11]. We estimate our difference from previous studies is primarily due to the use of rates instead of final stocks of mature ecosystems, as most restored sites would not reach maturity by 2100 due to the gradual implementation of restoration over the twenty-first century and that certain ecosystem types (Extended Data Fig. 9) require >70 years to build up their carbon stock.

Our predicted amount thus forms an important but moderate contribution to reducing atmospheric CO_2 closer to pre-industrial levels by 2100. A more realistic role of ecosystem restoration may thus be to keep pace with future emissions. Shared Socioeconomic Pathways (SSPs) are widely applied scenarios for forecasting emissions that consider impacts of varied climate policies from a shift towards a sustainable green future (SSP1–2.6) to business as usual (SSP5–8.5)[46,47]. Combining the carbon benefit of global ecosystem restoration with emission trends of each SSP (SSP1–2.6: 169.6 Gt, SSP2–4.5: 642.4 Gt, SSP3–7.0: 1,319.4 Gt and SSP5–8.5: 1,989.0 Gt) suggests restoration has a limited mitigating effect without transformative global climate policies (Fig. 5). Anthropogenic contributions to the atmospheric carbon balance remain positive throughout the twenty-first century in SSP5–8.5 and SSP3–7.0 even with restoration site prioritization for carbon gain, and the proportion of total anthropogenic carbon burden can only be reduced by 3.7% (SSP5–8.5) or 5.0% (SSP3–7.0). Ecosystem restoration in SSP2–4.5 leads to zero annual emissions by 2100 (and a 7.6% reduction of the carbon burden), but this is insufficient to meet any reasonable climate target. SSP1–2.6 is the most difficult scenario to realize due to its dramatic global greening requirements of the industry, but its implementation with predicted restoration actions could reduce the atmospheric carbon burden by 12.0%. SSP1–2.6 entails zero and then negative emissions from the second half of the 2070s. Combined with global restoration, this threshold can be brought forward to the late 2060s. Prioritization of regions with the highest carbon gain affects this date only marginally. However, SSP1–2.6 also contains some NCS-based mitigation by afforestation[46], so the actual improvement of this pathway might be overestimated by simply adding all restoration-related sequestration to it.

Considering restoration possibilities and predicted ecosystem state transitions using climate projections, our model provides alarming results, as we predict a continuous loss of ecosystem-locked carbon, particularly in tropical forest regions, although carbon gains

https://doi.org/10.1038/s41561-025-01742-z

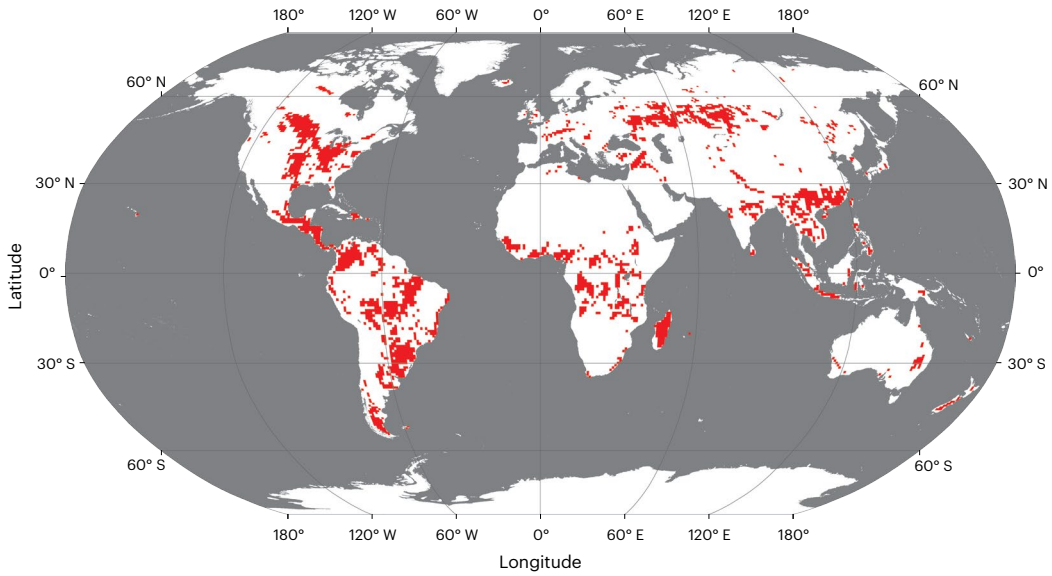

Fig. 4 | Distribution of the 2,675 priority regions for ecosystem restoration. Priority regions are 100 × 100 km pixels, covering 20% of all restorable land area with the highest possible carbon gain. Priority regions do not necessarily require restoration in their entire area and certain amounts of the degraded areas may not be available for restoration. Restoration is not restricted to reforestation but is inclusive of any potential ecosystem type (that is, forest, shrubland, grassland, wetland or their mosaic) predicted to each region.

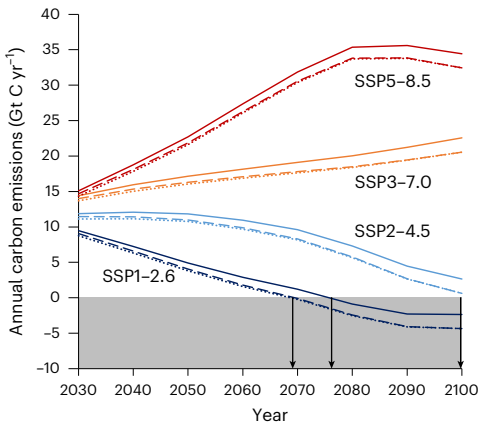

Fig. 5 | The effect of global ecosystem restoration on annual carbon emissions according to four future climate pathways. Solid line: no restoration, dashed line: restoration without prioritization, dotted line: restoration with site prioritization for carbon gain. Arrows point at the years when the global zero-emissions line is crossed, whereas the shaded area corresponds to negative emissions. In SSP1–2.6, we expect a pervasive shift towards sustainable green economies globally, whereas SSP2–4.5 is characterized by slower progress and little shift from the current socio-economic patterns. In contrast, SSP3–7.0 takes place if domestic and regional concerns about competitiveness and security hinder the global shift towards sustainability, and SSP5–8.5 will take place if we keep on relying on competitive markets and rapid technological progress to maintain a resource- and energy-intensive lifestyle all over the world[45]. Decimal numbers in the pathway names indicate expected radiative forcing values (expressed in W m^{-2}) in 2100.

are also expected at higher latitudes. Depending on the scenario, the rate of annual carbon emission is predicted to range from 0.11 to 0.64 Gt, in SSP1–26 and SSP5–8.5, respectively, with the other scenarios located between them. However, it is important to acknowledge the resilience of natural, functional ecosystems against state transitions[48], which thus may take place with some delay after underlying drivers exceeded their original rate of variability. Our findings highlight the importance of measures supporting ecosystem resilience (for example, promoting tree recruitment in forests threatened by climate change[49]) to delay state transitions[48] and concomitant carbon emissions. If this is sustained until all mitigation measures (including improved habitat management and industrial solutions) restore atmospheric CO_2 levels in a more distant future, unfavourable state transitions may be prevented. Furthermore, future climate scenarios probably contain novel climates that our model is inherently not trained for, reducing its reliability[50].

In sum, we demonstrated that terrestrial ecosystem restoration can play a role in climate change mitigation in the near future, if applied in conjunction with a prompt shift towards energy-efficient, renewable-based economies of SSP1–2.6 and if ecosystem state transitions are suppressed where possible and desirable. In other scenarios, the most appropriate aims of ecosystem restoration as an NCS will be around local to regional-scale climate change adaptation due to uncertainties related to global-scale mitigation. Optimizing restoration site selection for adaptation instead of mitigation would probably yield lower carbon capture, but the importance of ecosystem restoration in climate change adaptation cannot be overestimated for the livelihoods of local communities, especially those that are nature-reliant[51,52]. Intact ecosystems dampen the effects of heatwaves by optimal evapotranspiration rates[53], prevent soil erosion after increased precipitation events due to well-developed root systems[54] and increase the resilience of pollinator populations[55], which are threatened by climate change[56,57]. Due to the limited likelihood of any notable mitigation of climate change through global ecosystem restoration in the short or medium term, future policies should (1) prioritize adaptation and optimize restoration activities in favour of vulnerable peoples, (2) streamline mitigation plans by rigorous mechanisms to cut emissions instead of investing in offsetting with uncertain results[20,43] and (3) support the original goal of ecosystem restoration to combat the biodiversity crisis[58] and thereby increase the resilience of ecosystem services, rather than solely carbon sequestration.

Online content

Any methods, additional references, Nature Portfolio reporting summaries, source data, extended data, supplementary information, acknowledgements, peer review information; details of author contributions and competing interests; and statements of data and code availability are available at https://doi.org/10.1038/s41561-025-01742-z.

References

1. *Nature Restoration Law* (European Commission, 2023); https://environment.ec.europa.eu/topics/nature-and-biodiversity/nature-restoration-law_en
2. Holl, K. D. & Brancalion, P. H. Tree planting is not a simple solution. *Science* **368**, 580–581 (2020).
3. Fischer, J., Riechers, M., Loos, J., Martin-Lopez, B. & Temperton, V. M. Making the UN decade on ecosystem restoration a social-ecological endeavour. *Trends Ecol. Evol.* **36**, 20–28 (2021).
4. Smith, P. et al. Biophysical and economic limits to negative CO_2 emissions. *Nat. Clim. Change* **6**, 42–50 (2016).
5. Cook-Patton, S. C. et al. Protect, manage and then restore lands for climate mitigation. *Nat. Clim. Change* **11**, 1027–1034 (2021).
6. Nolan, C. J., Field, C. B. & Mach, K. J. Constraints and enablers for increasing carbon storage in the terrestrial biosphere. *Nat. Rev. Earth Environ.* **2**, 436–446 (2021).
7. Walker, W. S. et al. The global potential for increased storage of carbon on land. *Proc. Natl Acad. Sci. USA* **119**, e2111312119 (2022).
8. Fuss, S. et al. Betting on negative emissions. *Nat. Clim. Change* **4**, 850–853 (2014).
9. Bastin, J. F. et al. The global tree restoration potential. *Science* **365**, 76–79 (2019).
10. Strassburg, B. B. et al. Global priority areas for ecosystem restoration. *Nature* **586**, 724–729 (2020).
11. Lewis, S. L., Mitchard, E. T., Prentice, C., Maslin, M. & Poulter, B. Comment on 'the global tree restoration potential'. *Science* **366**, eaaz0388 (2019).
12. Veldman, J. W. et al. Comment on 'the global tree restoration potential'. *Science* **366**, eaay7976 (2019).
13. Tölgyesi, C. et al. Underground deserts below fertility islands? Woody species desiccate lower soil layers in sandy drylands. *Ecography* **43**, 848–859 (2020).
14. Aguirre-Gutiérrez, J., Stevens, N. & Berenguer, E. Valuing the functionality of tropical ecosystems beyond carbon. *Trends Ecol. Evol.* **38**, 1109–1111 (2023).
15. Dass, P., Houlton, B. Z., Wang, Y. & Warlind, D. Grasslands may be more reliable carbon sinks than forests in California. *Environ. Res. Lett.* **13**, 074027 (2018).
16. Pellegrini, A. F. et al. Soil carbon storage capacity of drylands under altered fire regimes. *Nat. Clim. Change* **13**, 1089–1094 (2023).
17. Stevens, N. & Bond, W. J. A trillion trees: carbon capture or fuelling fires? *Trends Ecol. Evol.* **39**, 1–4 (2024).
18. Zhou, Y. et al. Limited increases in savanna carbon stocks over decades of fire suppression. *Nature* **603**, 445–449 (2022).
19. Jackson, R. B. et al. Trading water for carbon with biological carbon sequestration. *Science* **310**, 1944–1947 (2005).
20. Tölgyesi, C., Buisson, E., Helm, A., Temperton, V. M. & Török, P. Urgent need for updating the slogan of global climate actions from 'tree planting' to 'restore native vegetation'. *Restor. Ecol.* **30**, e13594 (2022).
21. Wieczorkowski, J. D. & Lehmann, C. E. Encroachment diminishes herbaceous plant diversity in grassy ecosystems worldwide. *Glob. Change Biol.* **28**, 5532–5546 (2022).
22. Luyssaert, S. et al. Trade-offs in using European forests to meet climate objectives. *Nature* **562**, 259–262 (2018).
23. Rohatyn, S., Yakir, D., Rotenberg, E. & Carmel, Y. Limited climate change mitigation potential through forestation of the vast dryland regions. *Science* **377**, 1436–1439 (2022).
24. Pausas, J. G. & Bond, W. J. Alternative biome states in terrestrial ecosystems. *Trends Plant Sci.* **25**, 250–263 (2020).
25. Erdős, L. et al. How climate, topography, soils, herbivores, and fire control forest–grassland coexistence in the Eurasian forest-steppe. *Biol. Rev.* **97**, 2195–2208 (2022).
26. Mattos, C. R. et al. Double stress of waterlogging and drought drives forest–savanna coexistence. *Proc. Natl Acad. Sci. USA* **120**, e2301255120 (2023).
27. Doelman, J. C. & Stehfest, E. The risks of overstating the climate benefits of ecosystem restoration. *Nature* **609**, E1–E3 (2022).
28. Mo, L. et al. Integrated global assessment of the natural forest carbon potential. *Nature* **624**, 92–101 (2023).
29. Williams, B. A. et al. Global potential for natural regeneration in deforested tropical regions. *Nature* **636**, 131–137 (2024).
30. IPBES in *Global Assessment Report on Biodiversity and Ecosystem Services of the Intergovernmental Science-Policy Platform on Biodiversity and Ecosystem Services* (eds Brondizio, E. S. et al.) (IPBES Secretariat, 2019).
31. Zhang, J., Ma, K. & Fu, B. Wetland loss under the impact of agricultural development in the Sanjiang Plain, NE China. *Environ. Monit. Assess.* **166**, 139–148 (2010).
32. Mitchell, M. E. et al. Potential of water quality wetlands to mitigate habitat losses from agricultural drainage modernization. *Sci. Total Environ.* **838**, 156358 (2022).
33. Anadón, J. D., Sala, O. E. & Maestre, F. T. Climate change will increase savannas at the expense of forests and treeless vegetation in tropical and subtropical Americas. *J. Ecol.* **102**, 1363–1373 (2014).
34. Xu, X., Jia, G., Zhang, X., Riley, W. J. & Xue, Y. Climate regime shift and forest loss amplify fire in Amazonian forests. *Glob. Change Biol.* **26**, 5874–5885 (2020).
35. Flores, B. M. et al. Critical transitions in the Amazon forest system. *Nature* **626**, 555–564 (2024).
36. Zeng, Y. et al. Economic and social constraints on reforestation for climate mitigation in Southeast Asia. *Nat. Clim. Change* **10**, 842–844 (2020).
37. Weber, J. et al. Chemistry-albedo feedbacks offset up to a third of forestation's CO_2 removal benefits. *Science* **383**, 860–864 (2024).
38. Ratnam, J. et al. Trees as nature-based solutions: a global south Perspective. *One Earth* **3**, 140–144 (2020).
39. Fleischman, F. et al. Restoration prioritization must be informed by marginalized people. *Nature* **607**, E5–E6 (2022).
40. Temperton, V. M. et al. Step back from the forest and step up to the Bonn Challenge: how a broad ecological perspective can promote successful landscape restoration. *Restor. Ecol.* **27**, 705–719 (2019).
41. Heilmayr, R., Echeverría, C. & Lambin, E. F. Impacts of Chilean forest subsidies on forest cover, carbon and biodiversity. *Nat. Sustain.* **3**, 701–709 (2020).
42. Ramprasad, V., Joglekar, A. & Fleischman, F. Plantations and pastoralists: afforestation activities make pastoralists in the Indian Himalaya vulnerable. *Ecol. Soc.* **25**, 1 (2020).
43. Fleischman, F. et al. Pitfalls of tree planting show why we need people-centered natural climate solutions. *BioScience* **70**, 947–950 (2020).
44. Coleman, E. A. et al. Limited effects of tree planting on forest canopy cover and rural livelihoods in Northern India. *Nat. Sustain.* **4**, 997–1004 (2021).
45. Potapov, P. et al. Global maps of cropland extent and change show accelerated cropland expansion in the twenty-first century. *Nat. Food* **3**, 19–28 (2022).
46. Riahi, K. et al. The Shared Socioeconomic Pathways and their energy, land use, and greenhouse gas emissions implications: an overview. *Glob. Environ. Change* **42**, 153–168 (2017).
47. Gidden, M. J. et al. Global emissions pathways under different socioeconomic scenarios for use in CMIP6: a dataset of harmonized emissions trajectories through the end of the century. *Geosci. Model Dev.* **12**, 1443–1475 (2019).

48. Sardanyés, J., Ivančić, F. & Vidiella, B. Identifying regime shifts, transients and late warning signals for proactive ecosystem management. *Biol. Conserv.* **290**, 110433 (2024).
49. Stevens-Rumann, C. S. et al. Evidence for declining forest resilience to wildfires under climate change. *Ecol. Lett.* **21**, 243–252 (2018).
50. Bede-Fazekas, Á. & Somodi, I. Precipitation and temperature timings underlying bioclimatic variables rearrange under climate change globally. *Glob. Change Biol.* **30**, e17496 (2024).
51. Munang, R. et al. Climate change and ecosystem-based adaptation: a new pragmatic approach to buffering climate change impacts. *Curr. Opin. Environ. Sustain.* **5**, 67–71 (2013).
52. Díaz, S. et al. Assessing nature's contributions to people. *Science* **359**, 270–272 (2018).
53. Drake, J. E. et al. Trees tolerate an extreme heatwave via sustained transpirational cooling and increased leaf thermal tolerance. *Glob. Change Biol.* **24**, 2390–2402 (2018).
54. Liu, H. et al. Nature-based framework for sustainable afforestation in global drylands under changing climate. *Glob. Change Biol.* **28**, 2202–2220 (2022).
55. Kaiser-Bunbury, C. N. et al. Ecosystem restoration strengthens pollination network resilience and function. *Nature* **542**, 223–227 (2017).
56. Vanbergen, A. J. & Initiative, T. I. P. Threats to an ecosystem service: pressures on pollinators. *Front. Ecol. Environ.* **11**, 251–259 (2013).
57. Settele, J., Bishop, J. & Potts, S. G. Climate change impacts on pollination. *Nat. Plants* **2**, 16092 (2016).
58. Staude, I. R. et al. Prioritize grassland restoration to bend the curve of biodiversity loss. *Restor. Ecol.* **31**, e13931 (2023).

[1]MTA-SZTE 'Momentum' Applied Ecology Research Group, University of Szeged, Szeged, Hungary. [2]HUN-REN-UD Functional and Restoration Ecology Research Group, Debrecen, Hungary. [3]HUN-REN Centre for Agricultural Research, Institute for Soil Sciences, Budapest, Hungary. [4]Institute of Ecology, School of Sustainability, Leuphana University Lüneburg, Lüneburg, Germany. [5]Avignon Univ, Aix Marseille Univ, CNRS, IRD, IMBE, Avignon, France. [6]Department of Genetics, Ecology and Evolution, Federal University of Minas Gerais, Belo Horizonte, Brazil. [7]Taxonomy and Macroecology, Royal Botanic Garden Edinburgh, Edinburgh, UK. [8]School of GeoSciences, University of Edinburgh, Edinburgh, UK. [9]University of Debrecen, Department of Ecology, Debrecen, Hungary. [10]Balaton Limnological Research Institute, Tihany, Hungary. [11]Department of Ecology, University of Szeged, Szeged, Hungary. [12]HUN-REN Centre for Ecological Research, Institute of Ecology and Botany, Vácrátót, Hungary. [13]Department of Environmental and Landscape Geography, Institute of Geography and Earth Sciences, ELTE Eötvös Loránd University, Budapest, Hungary. [14]These authors contributed equally: Csaba Tölgyesi, Nándor Csikós. ✉e-mail: festuca7@yahoo.com

Methods

Model construction

Ecosystem restoration can have a large variety of goals and natural target vegetation states. For modelling purposes, we narrowed these down to four broad ecosystem types: forest, shrubland, grassland and wetland. These are also listed among the major land-cover categories of Earth in the Copernicus Global Land Service–Land Cover raster and available as fractional scores in pixels of 1-ha resolution (version 2019)[59] (A in Fig. 1). Other land-cover categories in the database correspond to either non-target ecosystem types for classical restoration (cropland and built-up areas; but see Elmqvist et al.[60] and Klaus and Kiehl[61] for urban restoration initiatives) or natural ecosystem types with little vegetation and therefore minor carbon sequestration rates (bare/sparse vegetation, snow and ice and moss and lichen).

To construct a predictive model for the potential global cover distribution of the four selected ecosystem types, we followed modelling principles in Bastin et al.[9] For learning sites (that is, pixels with known fractional cover scores of target ecosystems and environmental predictors), we used their 78.850 pixels (100 m × 100 m) supplemented with 20.000 more pixels with non-zero fractional cover percentages for each ecosystem type (80.000 additional pixels in total) in protected areas worldwide (except Antarctica) (B in Fig. 1). These latter pixels were selected by first assigning every pixel in protected areas that contained at least one of the target ecosystem types to a pool of each ecosystem type (pixels could be allocated to more than one pool if they contained more than one target ecosystem type), then we randomly selected (without repetition) 20.000 pixels from each pool, leading to 158.850 pixels in total (Extended Data Fig. 6).

Fractional cover scores were kept for subsequent model construction, so pool assignment did not mean that a pixel was fully attributed to an ecosystem type. The four pools were needed to enable similar representations of each ecosystem type in the final set of learning sites. We used the World Database on Protected Areas[62] for the delineation of protected areas. We included all listed protected areas (for example, EU Natura 2000 areas) and did not restrict pixel selection to strict nature reserves, as that procedure would exclude sustainable coexistence of humans with nature, such as extensive grassland management or silvopastoral systems, which can also lead to high biodiversity and co-benefits for climate change mitigation/adaptation and are often practical targets of restoration efforts[63]. Thus, our approach includes components of land sharing and land sparing.

We allocated ten environmental predictors, including five climatic (WorldClim database[64]; 1 km × 1 km resolution), three edaphic (SoilGrids250m[65]; 250 m × 250 m) and two topographic (GMTED2010[66]; 250 m × 250 m) variables (Extended Data Fig. 9) to every learning site (Supplementary Table 1) (C in Fig. 1). These environmental variables proved to be reliable predictors in Bastin et al.[9]. The differences in the spatial resolution of the variables were handled with the bilinear resampling technique of ESRI ArcMap 10.8. The bilinear resampling technique involves attributing the average value of the four nearest pixels within a 2 × 2 window to the relevant output pixel. This process follows a bilinear mathematical function along both the horizontal and vertical axes and is the commonly applied method for smoothly transitioning continuous datasets lacking clear boundaries[67].

We used Random Forest machine learning regression models with fivefold cross-validations[68] for training 500 trees of (potentially) unlimited depth (D in Fig. 1). The number of variables to possibly split at each node was set to three (that is, the default value for ten predictors). The models were evaluated by regressing observed values by predicted values (both of which were fractional)[69]. Spatial distribution of the model uncertainty was assessed by the standard deviation of the predictions made by the five trained sub-models originated from the fivefold cross-validation. According to the regression-based evaluation, the models of forest, shrubland and grassland had high predictive power ($0.70 < R^2 < 0.82$), although at high (above 60%) observed shrubland cover scores, the predictions tended to yield underestimations. This was due to the low prevalence of such pixels in the datasets (approximately 0.1%), but because they are rare, uncertainties in their range do not affect the overall predicted amount of shrubland (Extended Data Fig. 7). The model for wetlands was fair ($R^2 = 0.32$), with uncertainties also caused by the rarity of high empirical cover scores. Models' uncertainty, estimated using standard deviations, was evenly distributed across continents and biogeographic regions (Extended Data Fig. 8).

Predicting restoration targets

We predicted the potential forest, shrubland, grassland and wetland cover distributions as the ensemble mean of the five trained sub-models (according to the fivefold cross-validation) of each of the four ecosystem models to a global grid of 1 × 1 km cells (henceforth 'modelling sites') (E in Fig. 1). We also made predictions for a future period to take into account the effect of changing climate on the potential cover of ecosystem types, by updating the climatic predictors but leaving the non-climatic predictors unchanged. We chose the period 2061–2080 because it is in the middle of our study period (between 2030 and 2100). From among the global climate models of the Coupled Model Intercomparison Project Phase 6 (CMIP6)[70] having predictions in the WorldClim database[64], we selected EC-Earth3-Veg model[71], which has a medium (that is, 4.33) effective climate sensitivity value[72] and its predecessor (that is, EC-Earth) has been successfully used for carbon sequestration prediction[73]. Among the Shared Socioeconomic Pathways (SSPs), we considered SSP1–2.6, SSP2–4.5, SSP3–7.0 and SSP5–8.5.

The differences in the spatial resolution of the variables were handled with the bilinear resampling technique of ESRI ArcMap 10.8. Due to the independent construction of the four ecosystem models, the predicted total cover could exceed 100%. In such cases, we proportionately reduced the cover of each ecosystem type to sum up to 100% (for example, a prediction of 60% forest and 60% grassland was reduced to 50% each).

Once having the potential distribution of target ecosystems (in percentage fractions for every modelling site), we compared them to the present cover of the target ecosystems using the Copernicus Global Land Service–Land Cover raster (version 2019)[59]. We used the difference to identify degraded areas globally (F in Fig. 1).

However, built-up areas are rarely available for restoration purposes, so we removed them (their fractional cover from the modelling sites) from subsequent calculations. Likewise, restoration activities cannot be implemented in all agricultural areas due to their role in food security. Therefore, we identified intensive agricultural areas using the Land Use Systems of the World 1.1. database[74] and removed all corresponding modelling sites (G in Fig. 1). Fractional removal was not possible due to the data structure of the database. We considered the following categories as intensive agriculture: rain-fed crops, crops with moderate or higher livestock density, crops with high livestock density and large-scale irrigation agriculture.

It was common that a currently natural ecosystem type in a particular location is not the potential type in the future predictions, indicating that state transitions are expected worldwide in the near future. These can take place spontaneously but can also be assisted by landscape and conservation management (for example, to prevent catastrophic, pyric transitions from forests to savannahs by allowing a smooth transition with management). We did not lump them with restoration but handled them separately as 'state transitions', with additional (often negative) effects on carbon sequestration rates.

We finally had five potential cover values (one based on current and four based on future climates) for every target ecosystem type in all modelling sites, covering the terrestrial surface of Earth that is available for restoration (or prone to state transitions). Our model did not identify specific mosaic ecosystems (for example, savannah-forest mosaics) but handled them adequately, because the ecosystem-type cover values were proportional, meaning that such a modelling site,

for instance, contained certain proportions of forest, shrubland and grassland alike. These constituting ecosystem types were then used separately in subsequent carbon gain calculations.

Predicting carbon gain potential

As the next step, we assigned carbon sequestration rates (t ha^{-1} yr^{-1}) to the modelling sites. Carbon sequestration rates of a target ecosystem type can vary greatly among biomes (for example, tropical rainforest vs boreal forest). To account for this heterogeneity, we first removed all modelling sites located in polar or arid biomes using the 'Resolve EcoRegions2017' database[75] (H in Fig. 1), because these climates allow very low primary productivity and therefore low carbon sequestration rates. Then, we combined the four target ecosystem types with the remaining biomes listed in the database, resulting in 12 biome-specific ecosystem types: boreal forest, temperate forest, tropical/subtropical dry forest, tropical/subtropical moist forest, mangrove forest/shrubland, boreal/temperate shrubland (including heathland), tropical/subtropical shrubland, boreal/temperate grassland, tropical/subtropical grassland, boreal wetland (predominantly peatland), temperate wetland (including salt marshes) and tropical/subtropical wetland (I in Fig. 1). For boreal, temperate, tropical/subtropical dry forest and tropical/subtropical moist forests, we adopted the sequestration rates from Cook-Patton et al.[76], who compiled and summarized over ten thousand records from regenerating forests. They provided ecoregion-specific rates, which we averaged across our broader biome-specific forest ecosystem types. For open ecosystems, we heavily relied on the database of the European Environmental Agency[77]. For biome-specific ecosystem types that were not included in any of these databases or had a poor coverage in the European Environmental Agency's database, we searched for published literature records that considered total ecosystem carbon sequestration rates, including both above- and belowground biomass and soil organic carbon, except in tropical/subtropical grasslands, where frequent fires (and herbivory) preclude the formation of a stable aboveground carbon sink. So in their case, we used only records from belowground compartments (Extended Data Fig. 9 and J in Fig. 1).

Once having the carbon sequestration rates of the 12 biome-specific ecosystem types, we calculated the carbon sequestration rate of each modelling site after the implementation of restoration or the combination of restoration and state transitions in future-climate-based predictions (K in Fig. 1). To get the carbon gain potential of modelling sites, we calculated their current, pre-restoration sequestration rate (L in Fig. 1) and subtracted this from the post-restoration rate (plus state transition, where applicable) (M in Fig. 1). We assumed 0 t C ha^{-1} sequestration to non-target ecosystem types (for example, bare soil surface and snow and ice). In a few rare cases we predicted negative carbon gain based on current climates, which can happen if, for example, current forest cover is locally higher for some reason than predicted by our model. We ignored these rare cases but negative rates owing to state transitions in future-climate-based predictions were retained. We used carbon gain values based on current climates to estimate the impact of ecosystem restoration on carbon emissions projected by Shared Socioeconomic Pathways (SSP1–2.6, SSP2–4.5, SSP3–7.0, SSP5–8.5) between 2030 and 2100 (SSP Public Database 2.0[46]).

Besides the global sequestration potential until 2100, we also identified priority regions for restoration where the highest carbon gain can be achieved first. Selecting the modelling sites with the top carbon gain values is a possible option, but they may be scattered across the world and due to their relatively small size are not especially suitable for planning global restoration strategies. Therefore, we used a coarser global grid of 100 × 100 km cells (22.880 cells in total). We ranked these large grid cells according to their total potential carbon gain as the summed values from the included modelling sites and set the cut-off at that rank above which the cells contained 20% of all restorable land area, that is, the 80th percentile. This way, we identified regions where the highest carbon sequestration can be achieved until 2030, which was set as a milestone year to restore the first 20% of the available land. This selection method yielded 2,669 priority regions (corresponding to 11.7% of all grid cells). We performed prioritization using only the present-climate-based predictions, because of the very low overall carbon gains predicted when future climates were considered.

Data preparation and model construction were done in ESRI ArcMap 10.8 and R 4.2.0 statistical software, respectively. We used the R packages 'groupdata2', 'ranger', 'raster' and 'sf' for model construction and predictions.

Limitations of the model

Using carbon sequestration rates instead of the carbon stocks of mature stands is a major improvement of our model compared to previous ones, but we used linear functions, although deviations from this can happen during stand maturation in some ecosystem types[78]. The lack of global data across different biomes precluded us from taking into account these nonlinearities. Our input dataset structure allowed us to consider restoration actions that entailed a change in vegetation or ecosystem type through the restoration, although this is not a prerequisite for ecosystem restoration and for carbon gain (for example, restoration of intensively managed grasslands to natural grasslands or tree plantations to forests, although these actions are sometimes difficult to distinguish from improved management). However, using proportional ecosystem type cover values alleviated this deficiency in mosaic ecosystems if the degradation manifested in changes in the proportions of constituting ecosystem types; so, for example, our model included the restoration of degraded savannah-forest mosaics to pristine ones with the original ecosystem-type cover proportions. Furthermore, future changes of some input data and other relevant trends (for example, changes in the area of intensive agriculture, biome boundary shifts and the effects of elevating CO_2 and changing climate in general on assimilation, decomposition, fire frequency) were not taken into account due to high uncertainties, but this also gives room for future research. Lastly, the 1-km^2 model resolution does not mean that the output maps are directly usable for local-scale restoration planning because the predictors are often extrapolated values that are not sensitive enough to fine-scale environmental heterogeneity (topography, soil and so on), which cannot be ignored in small-scale planning.

Data availability

Data used in this study are available in Extended Data Fig. 9 and Extended Data Table 1, Supplementary Data Table 1 and in the free databases cited. Processed data and models are available via Dryad at https://doi.org/10.5061/dryad.ksn02v7g4 (ref. 79). Source data are provided with this paper.

Code availability

R codes to prepare the models are available via Dryad at https://doi.org/10.5061/dryad.ksn02v7g4 (ref. 79).

References

59. Buchhorn, M. et al. Copernicus Global Land Service: land cover 100 m: collection 3: epoch 2019: globe (V3.0.1). *Zenodo* https://doi.org/10.5281/zenodo.3939038 (2020).
60. Elmqvist, T. et al. Benefits of restoring ecosystem services in urban areas. Current Opinion in. *Environ. Sustain.* **14**, 101–108 (2015).
61. Klaus, V. H. & Kiehl, K. A conceptual framework for urban ecological restoration and rehabilitation. *Basic Appl. Ecol.* **52**, 82–94 (2021).
62. UNEP-WCMC and IUCN *Protected Planet: The World Database on Protected Areas (WDPA)* (UNEP-WCMC, 2019); www.protectedplanet.net

63. Lyons, K. G. et al. Challenges and opportunities for grassland restoration: a global perspective of best practices in the era of climate change. *Glob. Ecol. Conserv.* **46**, e02612 (2023).
64. Fick, S. E. & Hijmans, R. J. WorldClim 2: new 1-km spatial resolution climate surfaces for global land areas. *Int. J. Climatol.* **37**, 4302–4315 (2017).
65. Hengl, T. et al. SoilGrids250m: global gridded soil information based on machine learning. *PLoS ONEs* **12**, e0169748 (2017).
66. Danielson, J. J. & Gesch, D. B. *Global Multi-Resolution Terrain Elevation Data 2010 (GMTED2010)* Report No. OFR 2011-1073 (US Geological Survey, 2011).
67. Baboo, S. S. & Devi, M. R. An analysis of different resampling methods in Coimbatore, District. *Glob. J. Computer Sci. Technol.* **10**, 61–66 (2010).
68. Breiman, L. Random forests. *Mach. Learn.* **45**, 5–32 (2001).
69. Piñeiro, G., Perelman, S., Guerschman, J. P. & Paruelo, J. M. How to evaluate models: observed vs. predicted or predicted vs. observed? *Ecol. Modell.* **216**, 316–322 (2008).
70. Eyring, V. et al. Overview of the Coupled Model Intercomparison Project Phase 6 (CMIP6) experimental design and organization. *Geosci. Model Dev.* **9**, 1937–1958 (2016).
71. Döscher, R. et al. The EC-Earth3 earth system model for the coupled model intercomparison project 6. *Geosci. Model Dev.* **15**, 2973–3020 (2022).
72. Zelinka, M. D. et al. Causes of higher climate sensitivity in CMIP6 models. *Geophys. Res. Lett.* **47**, e2019GL085782 (2020).
73. Pechanec, V. et al. Modelling of the carbon sequestration and its prediction under climate change. *Ecol. Inform.* **47**, 50–54 (2018).
74. *Land Use Systems of the World* (FAO, 2010); https://data.apps.fao.org/map/catalog/srv/eng/catalog.search#/metadata/fc32c5de-440c-46aa-9cad-81f4c8b84c6a
75. Dinerstein, E. et al. An ecoregion-based approach to protecting half the terrestrial realm. *BioScience* **67**, 534–545 (2017).
76. Cook-Patton, S. C. et al. Mapping carbon accumulation potential from global natural forest regrowth. *Nature* **585**, 545–550 (2020).
77. *Carbon storage in EU terrestrial and marine ecosystems — European Environment Agency* (EEA, 2022); https://www.eea.europa.eu/data-and-maps/data/carbon-storage-in-global-terrestrial
78. Zhou, T. et al. Age-dependent forest carbon sink: estimation via inverse modeling. *J. Geophys. Res.: Biogeosci.* **120**, 2473–2492 (2015).
79. Tölgyesi, C. et al. Global ecosystem restoration has unexpectedly low potential to mitigate climate change. *Dryad* https://doi.org/10.5061/dryad.ksn02v7g4 (2025).
80. Page, S. E. et al. A record of Late Pleistocene and Holocene carbon accumulation and climate change from an equatorial peat bog (Kalimantan, Indonesia): implications for past, present and future carbon dynamics. *J. Quat. Sci.* **19**, 625–635 (2004).
81. Saunders, M. J., Jones, M. B. & Kansiime, F. Carbon and water cycles in tropical papyrus wetlands. *Wetlands Ecol. Manage.* **15**, 489–498 (2007).
82. Bernal, B. & Mitsch, W. J. A comparison of soil carbon pools and profiles in wetlands in Costa Rica and Ohio. *Ecol. Eng.* **34**, 311–323 (2008).
83. Lü, X. T., Yin, J. X., Jepsen, M. R. & Tang, J. W. Ecosystem carbon storage and partitioning in a tropical seasonal forest in Southwestern China. *For. Ecol. Manage.* **260**, 1798–1803 (2010).
84. Adame, M. F. et al. Carbon stocks and soil sequestration rates of tropical riverine wetlands. *Biogeosciences* **12**, 3805–3818 (2015).
85. Akpa, S. I., Odeh, I. O., Bishop, T. F., Hartemink, A. E. & Amapu, I. Y. Total soil organic carbon and carbon sequestration potential in Nigeria. *Geoderma* **271**, 202–215 (2016).
86. Hribljan, J. A., Suárez, E., Heckman, K. A., Lilleskov, E. A. & Chimner, R. A. Peatland carbon stocks and accumulation rates in the Ecuadorian páramo. *Wetland Ecol. Manage.* **24**, 113–127 (2016).
87. Kolka, R. K., Murdiyarso, D., Kauffman, J. B. & Birdsey, R. A. Tropical wetlands, climate, and land-use change: adaptation and mitigation opportunities. *Wetland Ecol. Manage.* **24**, 107–112 (2016).
88. Davila, A. & Bohlen, P. J. Hydro-ecological controls on soil carbon storage in subtropical freshwater depressional wetlands. *Wetlands* **41**, 66 (2021).
89. Sjögersten, S. et al. Coastal wetland ecosystems deliver large carbon stocks in tropical Mexico. *Geoderma* **403**, 115173 (2021).
90. Black, T. A. et al. Annual cycles of water vapor and carbon dioxide fluxes in and above a boreal aspen forest. *Glob. Change Biol.* **2**, 219–229 (1996).
91. Frolking, S. et al. Modelling temporal variability in the carbon balance of a spruce/moss boreal forest. *Glob. Change Biol.* **2**, 343–366 (1996).
92. Yarie, J. & Billings, S. Carbon balance of the taiga forest within Alaska: present and future. *Can. J. For. Res.* **32**, 757–767 (2002).
93. Röser, C. et al. Net CO_2 exchange rates in three different successional stages of the 'Dark Taiga' of central Siberia. *Tellus B: Chem. Phys. Meteorol.* **54**, 642–654 (2002).
94. Suni, T. et al. Vesala, Interannual variability and timing of growing-season CO_2 exchange in a boreal forest. *J. Geophys. Res.: Atmos.* **108**, D9 (2003).
95. Curtis, P. S. Biometric and eddy-covariance based estimates of annual carbon storage in five eastern North American deciduous forests. *Agric. For. Meteorol.* **113**, 3–19 (2002).
96. Urrutia-Jalabert, R., Malhi, Y. & Lara, A. The oldest, slowest rainforests in the world? Massive biomass and slow carbon dynamics of *Fitzroya cupressoides* temperate forests in southern Chile. *PLoS ONE* **10**, e0137569 (2015).
97. Parada, T., Lusk, C. H. & Donoso, P. J. Evidence that emergent *Nothofagus dombeyi* do not depress carbon sequestration rates of canopy species in an old-growth Chilean temperate forest. *N.Z. J. Bot.* **56**, 311–322 (2018).
98. Gough, C. M., Vogel, C. S., Harrold, K. H., George, K. & Curtis, P. S. The legacy of harvest and fire on ecosystem carbon storage in a north temperate forest. *Glob. Change Biol.* **13**, 1935–1949 (2007).
99. Michelsen, A., Andersson, M., Jensen, M., Kjøller, A. & Gashew, M. Carbon stocks, soil respiration and microbial biomass in fire-prone tropical grassland, woodland and forest ecosystems. *Soil Biol. Biochem.* **36**, 1707–1717 (2004).
100. Vargas, R., Allen, M. F. & Allen, E. B. Biomass and carbon accumulation in a fire chronosequence of a seasonally dry tropical forest. *Glob. Change Biol.* **14**, 109–124 (2008).
101. Coetsee, C., Gray, E. F., Wakeling, J., Wigley, B. J. & Bond, W. J. Low gains in ecosystem carbon with woody plant encroachment in a South African savanna. *J. Trop. Ecol.* **29**, 49–60 (2013).
102. Cao, S., Sanchez-Azofeifa, G. A., Duran, S. M. & Calvo-Rodriguez, S. Estimation of aboveground net primary productivity in secondary tropical dry forests using the Carnegie–Ames–Stanford approach (CASA) model. *Environ. Res. Lett.* **11**, 075004 (2016).
103. Pereira Júnior, L. R. Carbon stocks in a tropical dry forest in Brazil. *Rev. Cienc. Agron.* **47**, 32–40 (2016).
104. Abreu et al. The biodiversity cost of carbon sequestration in tropical savanna. *Sci. Adv.* **3**, e1701284 (2017).
105. Pelletier, J. et al. Carbon sink despite large deforestation in African tropical dry forests (miombo woodlands). *Environ. Res. Lett.* **13**, 094017 (2018).
106. Calvo-Rodriguez, S., Sanchez-Azofeifa, G. A., Duran, S. M., Do Espirito-Santo, M. M. & Ferreira Nunes, Y. R. Dynamics of carbon accumulation in tropical dry forests under climate change extremes. *Forests* **12**, 106 (2021).
107. Maia, V. A. et al. The carbon sink of tropical seasonal forests in southeastern Brazil can be under threat. *Sci. Adv.* **6**, eabd4548 (2020).

108. Yadav, V. S. et al. Carbon sequestration potential and CO_2 fluxes in a tropical forest ecosystem. *Ecol. Eng.* **176**, 106541 (2022).
109. Houghton, R. A. The annual net flux of carbon to the atmosphere from changes in land use 1850–1990. *Tellus B* **51**, 298–313 (1999).
110. DeFries, R. S. et al. Carbon emissions from tropical deforestation and regrowth based on satellite observations for the 1980s and 1990s. *Proc. Natl Acad. Sci. USA* **99**, 14256–14261 (2002).
111. Hamilton, J. G. et al. Forest carbon balance under elevated CO_2. *Oecologia* **131**, 250–260 (2002).
112. Nascimento, H. E. & Laurance, W. F. Total aboveground biomass in central Amazonian rainforests: a landscape-scale study. *For. Ecol. Manage.* **168**, 311–321 (2002).
113. Lasco, R. D. & Pulhin, F. B. Philippine forest ecosystems and climate change: carbon stocks, rate of sequestration and the Kyoto Protocol. *Ann. Trop. Res.* **25**, 37–52 (2003).
114. Gibbs, H. K., Brown, S., Niles, J. O. & Foley, A. Monitoring and estimating tropical forest carbon stocks: making REDD a reality. *Environ. Res. Lett.* **2**, 045023 (2007).
115. Sierra, C. A. et al. Total carbon stocks in a tropical forest landscape of the Porce region, Colombia. *For. Ecol. Manage.* **243**, 299–309 (2007).
116. Lewis, S. L. et al. Increasing carbon storage in intact African tropical forests. *Nature* **457**, 1003–1006 (2009).
117. Malhi, Y. & Grace, J. Tropical forests and atmospheric carbon dioxide. *Trends Ecol. Evol.* **15**, 332–337 (2000).
118. Ngo, K. M. et al. Carbon stocks in primary and secondary tropical forests in Singapore. *For. Ecol. Manage.* **296**, 81–89 (2013).
119. Wheeler, C. E. et al. Carbon sequestration and biodiversity following 18 years of active tropical forest restoration. *For. Ecol. Manage.* **373**, 44–55 (2016).
120. Zaragoza, M. J. G., Aranico, E. C., Tampus, A. D. & Amparado, R. F. Jr Carbon stock assessment of three different vegetative covers in Kapatagan, Lanao del Norte, Philippines. *Adv. Environ. Sci.* **8**, 205–220 (2016).
121. Ray, R. et al. Carbon sequestration and annual increase of carbon stock in a mangrove forest. *Atmos. Environ.* **45**, 5016–5024 (2011).
122. Alongi, D. M. Carbon sequestration in mangrove forests. *Carbon Manage.* **3**, 313–322 (2012).
123. Alongi, D. M. Carbon cycling and storage in mangrove forests. *Annu. Rev. Mar. Sci.* **6**, 195–219 (2014).
124. Kauffman, J. B., Heider, C., Norfolk, J. & Payton, F. Carbon stocks of intact mangroves and carbon emissions arising from their conversion in the Dominican Republic. *Ecol. Appl.* **24**, 518–527 (2014).
125. Gnanamoorthy, P. et al. Soil organic carbon stock in natural and restored mangrove forests in Pichavaram south-east coast of India. *Indian J. Geo Mar. Sci.* **48**, 801–808 (2019).
126. Adame et al. Future carbon emissions from global mangrove forest loss. *Glob. Change Biol.* **27**, 2856–2866 (2021).
127. Luo, H. et al. Mature semiarid chaparral ecosystems can be a significant sink for atmospheric carbon dioxide. *Glob. Change Biol.* **13**, 386–396 (2007).
128. Robinson, D. Implications of a large global root biomass for carbon sink estimates and for soil carbon dynamics. *Proc. R. Soc. B: Biol. Sci.* **274**, 2753–2759 (2007).
129. Beier, C. et al. Carbon and nitrogen balances for six shrublands across Europe. *Glob. Biogeochem. Cycles* **23**, GB4008 (2009).
130. Ruiz-Peinado, R., Moreno, G., Juarez, E., Montero, G. & Roig, S. The contribution of two common shrub species to aboveground and belowground carbon stock in Iberian dehesas. *J. Arid Environ.* **91**, 22–30 (2013).
131. Stamati, F. E., Nikolaidis, N. P. & Schnoor, J. L. Modeling topsoil carbon sequestration in two contrasting crop production to set-aside conversions with RothC–Calibration issues and uncertainty analysis. *Agric. Ecosyst. Environ.* **165**, 190–200 (2013).
132. Nie, X. et al. Distribution and controlling factors of soil organic carbon storage in the northeast Tibetan shrublands. *J. Soils Sediments* **19**, 322–331 (2019).
133. Zhao, M. et al. Assessing the effects of ecological engineering on carbon storage by linking the CA-Markov and InVEST models. *Ecol. Indic.* **98**, 29–38 (2019).
134. Chen, X., Hutley, L. B. & Eamus, D. Carbon balance of a tropical savanna of northern Australia. *Oecologia* **137**, 405–416 (2003).
135. Hutley, L. B., Leuning, R., Beringer, J. & Cleugh, H. A. The utility of the eddy covariance techniques as a tool in carbon accounting: tropical savanna as a case study. *Aust. J. Bot.* **53**, 663–675 (2005).
136. Grace, J., Jose, J. S., Meir, P., Miranda, H. S. & Montes, R. A. Productivity and carbon fluxes of tropical savannas. *J. Biogeogr.* **33**, 387–400 (2006).
137. Blaser, W. J., Shanungu, G. K., Edwards, P. J. & Olde Venterink, H. Woody encroachment reduces nutrient limitation and promotes soil carbon sequestration. *Ecol. Evol.* **4**, 1423–1438 (2014).
138. Fei, X. et al. Eddy covariance and biometric measurement s show that a savanna ecosystem in Southwest China is a carbon sink. *Sci. Rep.* **7**, 41025 (2017).
139. Conant, R. T., Paustian, K. & Elliott, E. T. Grassland management and conversion into grassland: effects on soil carbon. *Ecol. Appl.* **11**, 343–355 (2001).
140. Derner, J. D., Boutton, T. W. & Briske, D. D. Grazing and ecosystem carbon storage in the North American Great Plains. *Plant Soil* **280**, 77–90 (2006).
141. Guzman, J. G. & Al-Kaisi, M. Landscape position and age of reconstructed prairies effect on soil organic carbon sequestration rate and aggregate associated carbon. *J. Soil Water Conserv.* **65**, 9–21 (2010).
142. DeLuca, T. H. & Zabinski, C. A. Prairie ecosystems and the carbon problem. *Front. Ecol. Environ.* **9**, 407–413 (2011).
143. Ampleman, M. D., Crawford, K. M. & Fike, D. A. Differential soil organic carbon storage at forb- and grass-dominated plant communities, 33 years after tallgrass prairie restoration. *Plant Soil* **374**, 899–913 (2014).
144. Salemme, R. K., Olson, K. R., Gennadiyev, A. N. & Kovach, R. G. Effects of land use change, cultivation, and landscape position on prairie soil organic carbon stocks. *Open J. Soil Sci.* **8**, 163–173 (2018).
145. Fisher, M. J. et al. Carbon storage by introduced deep-rooted grasses in the South American savannas. *Nature* **371**, 236–238 (1994).
146. Post, W. M. & Kwon, K. C. Soil carbon sequestration and land-use change: processes and potential. *Glob. Change Biol.* **6**, 317–327 (2006).
147. Archer, S. et al. (eds) in *Global Environmental Change in the Ocean and on Land* 359–373 (Terrapub, 2004).
148. Vågen, T. G., Lal, R. & Singh, B. R. Soil carbon sequestration in sub-Saharan Africa: a review. *Land Degrad. Dev.* **16**, 53–71 (2005).
149. Boutton, T. W., Liao, J. D., Filley, T. R. & Archer, S. R. Belowground carbon storage and dynamics accompanying woody plant encroachment in a subtropical savanna. *Soil Carbon Sequestration Greenhouse Eff.* **57**, 181–205 (2009).
150. Maia, S. M., Ogle, S. M., Cerri, C. E. & Cerri, C. C. Effect of grassland management on soil carbon sequestration in Rondônia and Mato Grosso states, Brazil. *Geoderma* **149**, 84–91 (2009).
151. Räsänen, M. et al. Carbon balance of a grazed savanna grassland ecosystem in South Africa. *Biogeosciences* **14**, 1039–1054 (2017).
152. Awuah, J., Smith, S. W., Speed, J. D. & Graae, B. J. Can seasonal fire management reduce the risk of carbon loss from wildfires in a protected Guinea savanna? *Ecosphere* **13**, e4283 (2022).
153. Zhou, Y. Soil carbon in tropical savannas mostly derived from grasses. *Nat. Geosci.* **16**, 710–716 (2023).

Acknowledgements
C.T., Z.B. and P.T. were supported by the NKFIH K 146137, FK 142428 and KKP 144068 grants, respectively. The support of the János Bolyai Research Scholarship of the Hungarian Academy of Sciences and the New National Excellence Program of the Ministry for Culture and Innovation from the source of the National Research, Development and Innovation Fund (ÚNKP-23-5-SZTE-697) are also acknowledged. V.M.T. was supported by the German Ministry for Education and Research (BMBF) and by the state of Lower Saxony. F.A.O.S. was supported by grants from FAPEMIG. Á.B.-F. was supported by the János Bolyai Research Scholarship of the Hungarian Academy of Sciences. This work has been implemented by the National Multidisciplinary Laboratory for Climate Change (RRF-2.3.1-21-2022-00014) project within the framework of Hungary's National Recovery and Resilience Plan supported by the Recovery and Resilience Facility of the European Union.

Author contributions
C.T. conceived the study, Á.B.-F. constructed the models, N.C., Á.B.-F. and C.T. made the predictions and prepared the figures, C.T. led the writing of the paper, and all authors critically contributed to the evaluation of the findings and editing the paper.

Competing interests
The authors declare no competing interests.

Additional information
Extended data is available for this paper at https://doi.org/10.1038/s41561-025-01742-z.

Supplementary information The online version contains supplementary material available at https://doi.org/10.1038/s41561-025-01742-z.

Correspondence and requests for materials should be addressed to Csaba Tölgyesi.

Peer review information *Nature Geoscience* thanks the anonymous reviewers for their contribution to the peer review of this work. Primary Handling Editor: Tom Richardson, in collaboration with the *Nature Geoscience* team.

https://doi.org/10.1038/s41561-025-01742-z

Extended Data Table 1 | Predictors used for model construction

Predictor type and source	Predictor
Climatic: WorldClim[64] (https://www.worldclim.org/data/bioclim.html)	1. Annual mean temperature (°C ×10) 2. Mean temperature of wettest quarter (°C × 10) 3. Annual precipitation (mm) 4. Precipitation seasonality (coefficient of variation) 5. Precipitation of the driest quarter of the year (mm)
Edaphic: SoilGrids250m[65] (https://soilgrids.org/)	6. Sand content in the top 15 cm of the soil (%) 7. Soil organic carbon stock (g m^{-2}) 8. Depth to bedrock (m)
GMTED2010[66] (https://topotools.cr.usgs.gov/gmted_viewer)	9. Slope (degree) 10. Elevation above sea level (m)

https://doi.org/10.1038/s41561-025-01742-z

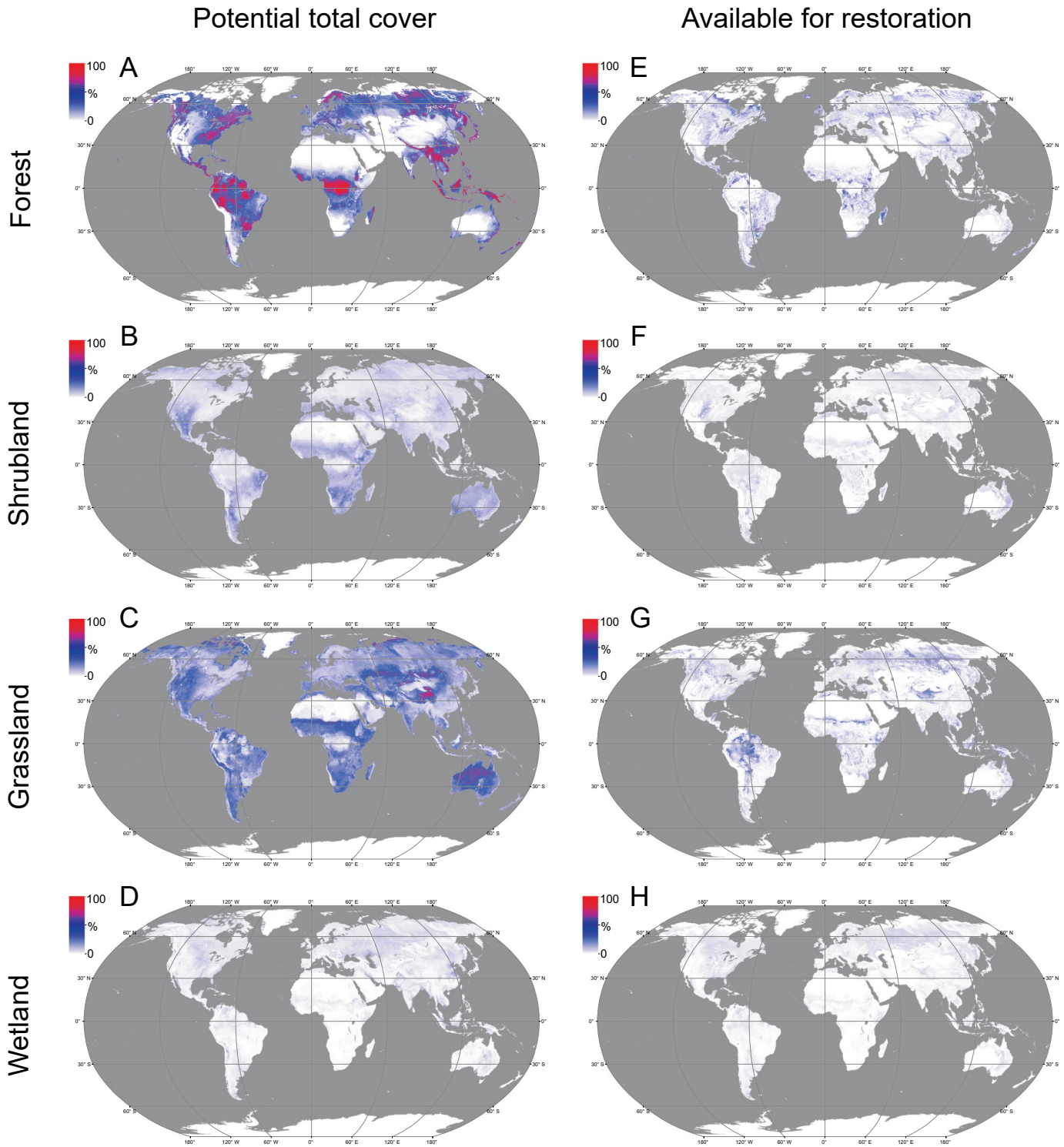

Extended Data Fig. 1 | Potential distribution of modelled ecosystems (A-D) and the available area for restoration or spontaneous establishment (E-H), predicted using SSP1-2.6 (2061–2080). Color coding indicates the percentage of each ecosystem type (predicted and available) within a 1 × 1 km grid. Thus, ecosystem combinations (for example forest steppes and savanna-forest mosaics) are also allowed in our grid-level restoration planning, although the proportion of each constituting ecosystem type appears on different maps. For example, a savanna-forest mosaic landscape can contain forested, shrubby and grassy parts within a grid cell, and their proportional values are shown on each of the three corresponding maps. We excluded potential restoration activities in intensive agricultural and built-up areas and in biomes with low productivity (polar and arid regions).

https://doi.org/10.1038/s41561-025-01742-z

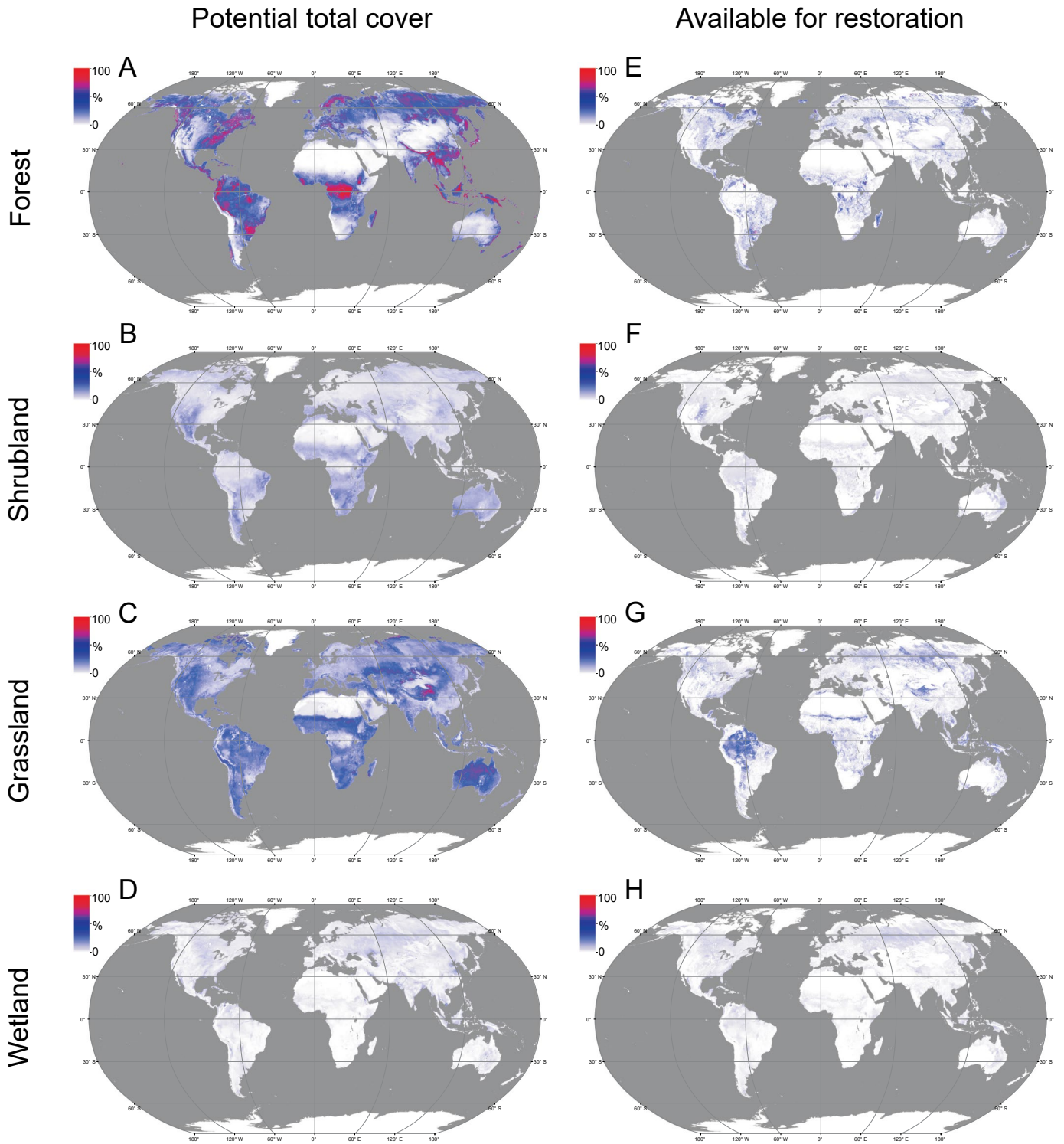

Extended Data Fig. 2 | Potential distribution of modelled ecosystems (A-D) and the available area for restoration or spontaneous establishment (E-H), predicted using SSP2-4.5 (2061–2080). Color coding indicates the percentage of each ecosystem type (predicted and available) within a 1 × 1 km grid. Thus, ecosystem combinations (for example forest steppes and savanna-forest mosaics) are also allowed in our grid-level restoration planning, although the proportion of each constituting ecosystem type appears on different maps. For example, a savanna-forest mosaic landscape can contain forested, shrubby and grassy parts within a grid cell, and their proportional values are shown on each of the three corresponding maps. We excluded potential restoration activities in intensive agricultural and built-up areas and in biomes with low productivity (polar and arid regions).

https://doi.org/10.1038/s41561-025-01742-z

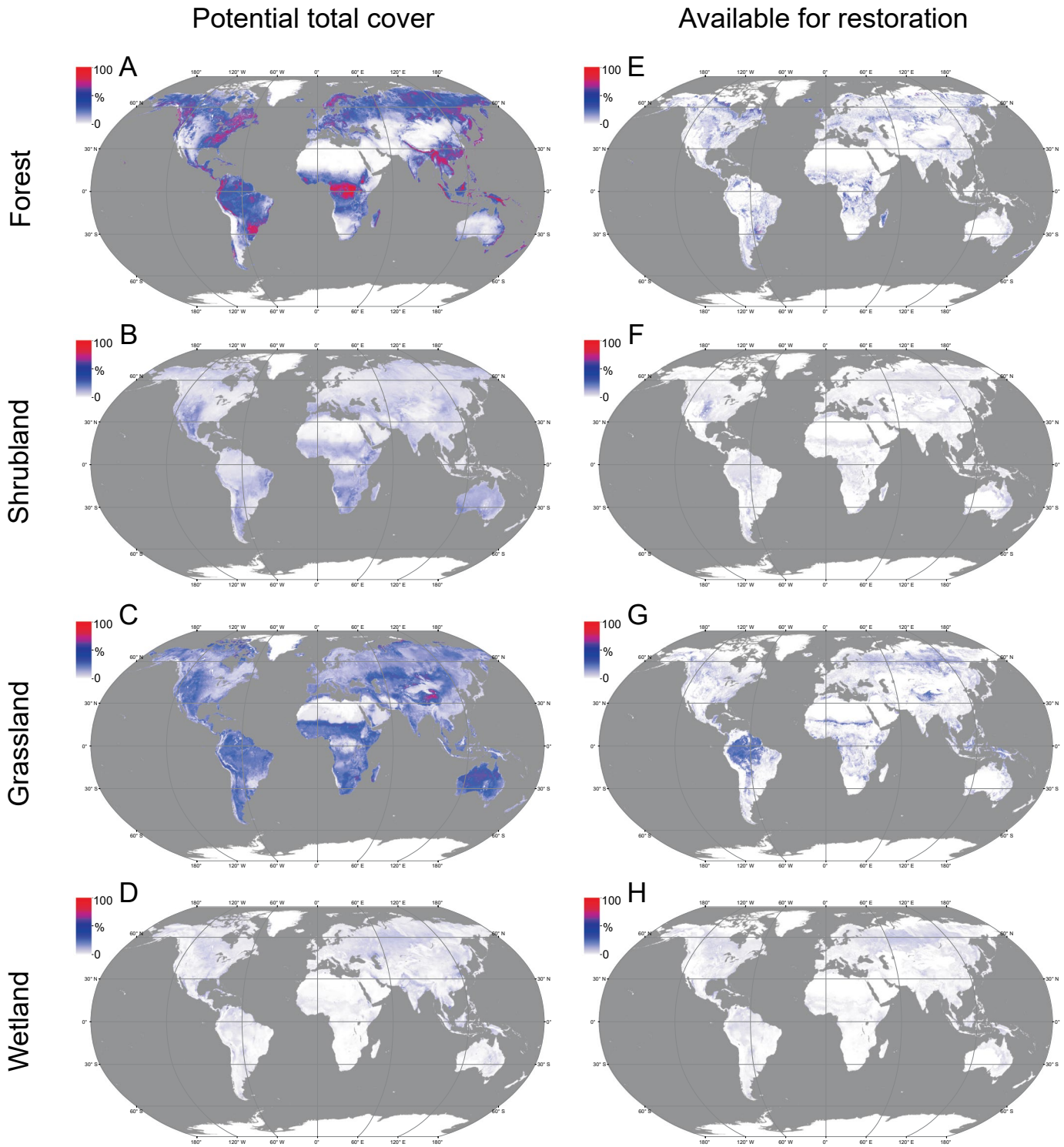

Extended Data Fig. 3 | 3 Potential distribution of modelled ecosystems (A-D) and the available area for restoration or spontaneous establishment (E-H), predicted using SSP3-7.0 (2061–2080). Color coding indicates the percentage of each ecosystem type (predicted and available) within a 1 × 1 km grid. Thus, ecosystem combinations (for example forest steppes and savanna-forest mosaics) are also allowed in our grid-level restoration planning, although the proportion of each constituting ecosystem type appears on different maps. For example, a savanna-forest mosaic landscape can contain forested, shrubby and grassy parts within a grid cell, and their proportional values are shown on each of the three corresponding maps. We excluded potential restoration activities in intensive agricultural and built-up areas and in biomes with low productivity (polar and arid regions).

https://doi.org/10.1038/s41561-025-01742-z

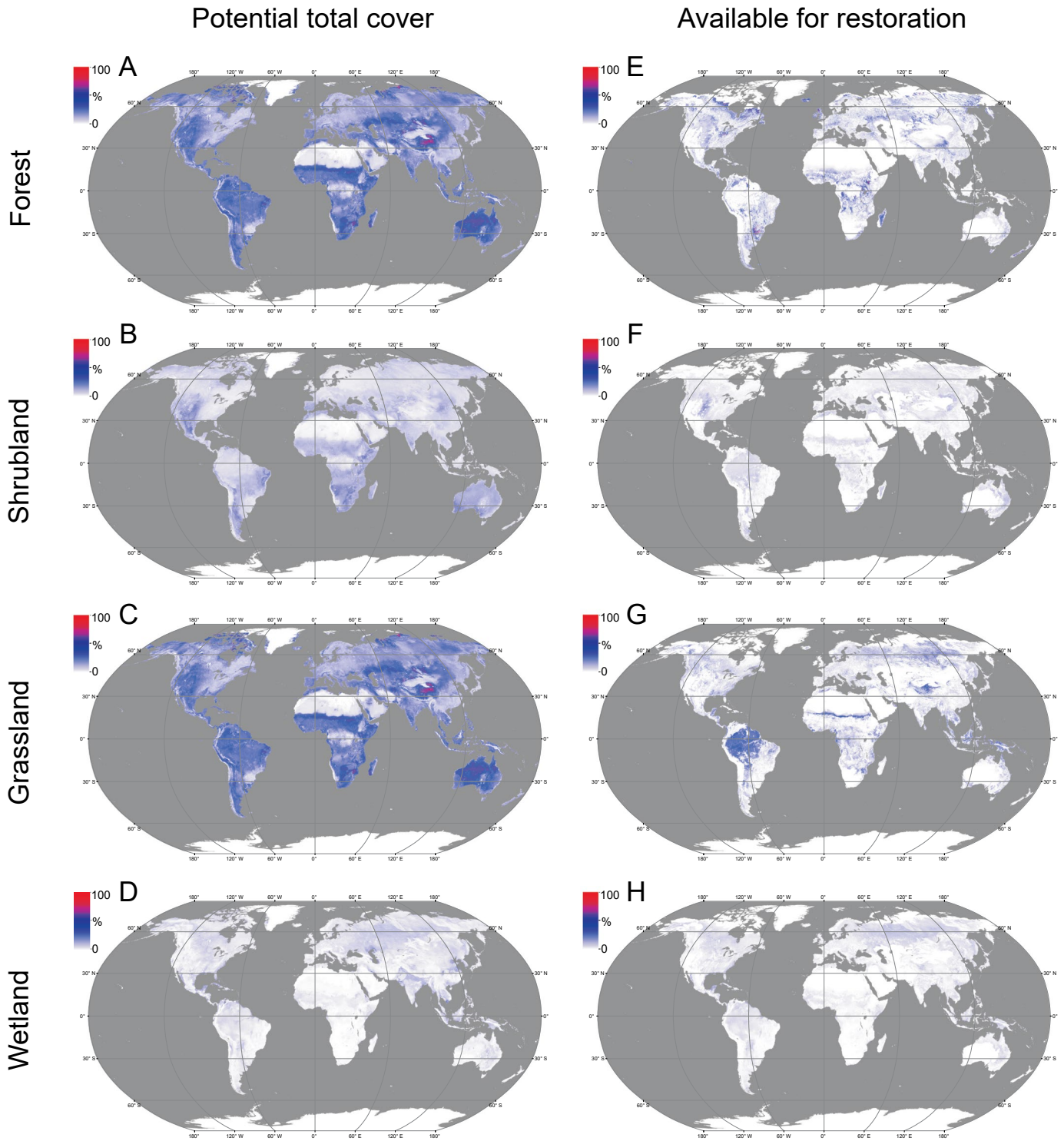

Extended Data Fig. 4 | Potential distribution of modelled ecosystems (A-D) and the available area for restoration or spontaneous establishment (E-H), predicted using SSP5-8.5 (2061–2080). Color coding indicates the percentage of each ecosystem type (predicted and available) within a 1 × 1 km grid. Thus, ecosystem combinations (for example forest steppes and savanna-forest mosaics) are also allowed in our grid-level restoration planning, although the proportion of each constituting ecosystem type appears on different maps. For example, a savanna-forest mosaic landscape can contain forested, shrubby and grassy parts within a grid cell, and their proportional values are shown on each of the three corresponding maps. We excluded potential restoration activities in intensive agricultural and built-up areas and in biomes with low productivity (polar and arid regions).

https://doi.org/10.1038/s41561-025-01742-z

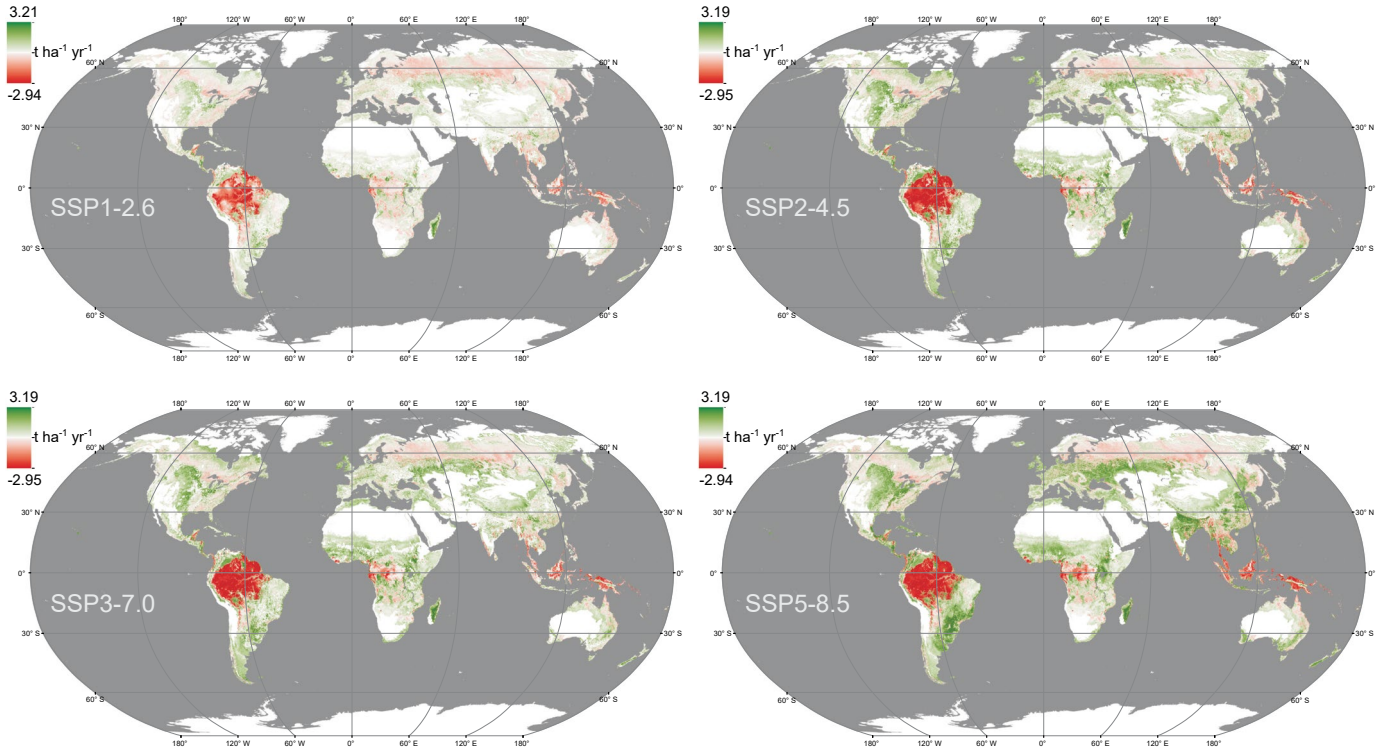

Extended Data Fig. 5 | Global distribution of potential annual rates of carbon gain (green) or loss (red). Calculations were made on all land available for restoration or subject to ecosystem state transitions, predicted using climates projected for 2061–2080 in scenarios SSP1-2.6, SSP2-4.5, SSP3-7.0, SSP5-8.5. Carbon gain or loss includes both above- and below-ground carbon capture (except in savanna grasslands where we considered only belowground rates due to frequent fires). Shown carbon gain rates are calculated as the difference between the rates of the predicted restoration targets minus the rates of the current ecosystem types in 1 × 1 km modeling sites. We used biome-specific rates for each of the four ecosystem types instead of global averages.

https://doi.org/10.1038/s41561-025-01742-z

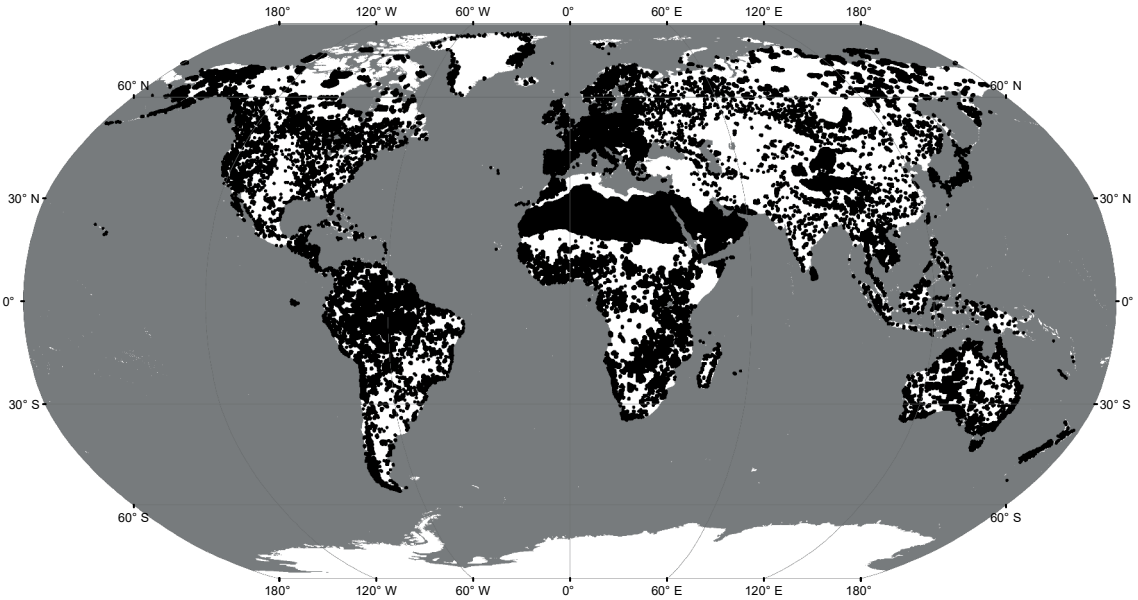

Extended Data Fig. 6 | Distribution of the 158.850 learning sites we used to train our predictive models for the four target ecosystem types. Located within protected areas, we assumed that they contain each ecosystem type in proportions that match restoration targets.

https://doi.org/10.1038/s41561-025-01742-z

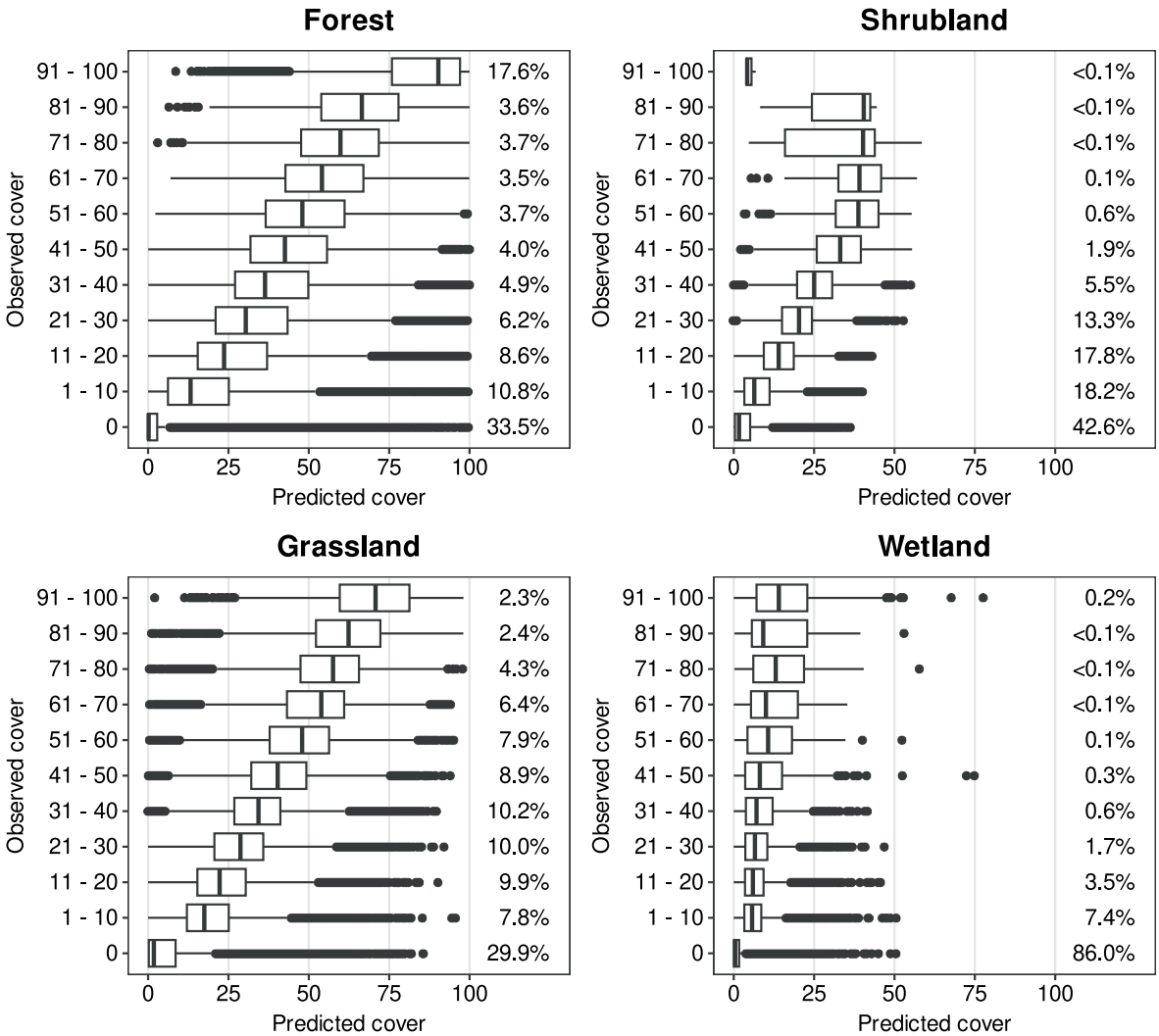

Extended Data Fig. 7 | Distribution of the predicted cover fraction values within eleven intervals of the observed values for each ecosystem type. Percentage scores in the right side of the subplots indicate the amount of pixels in the respective ranges. Boxes show the interquartile range (IQR) of the data. Thick lines in the boxes are the median values. Whiskers extend towards the minimum or maximum values but are no longer than 1.5 times the IQR. Data beyond the whiskers are shown as individual points.

https://doi.org/10.1038/s41561-025-01742-z

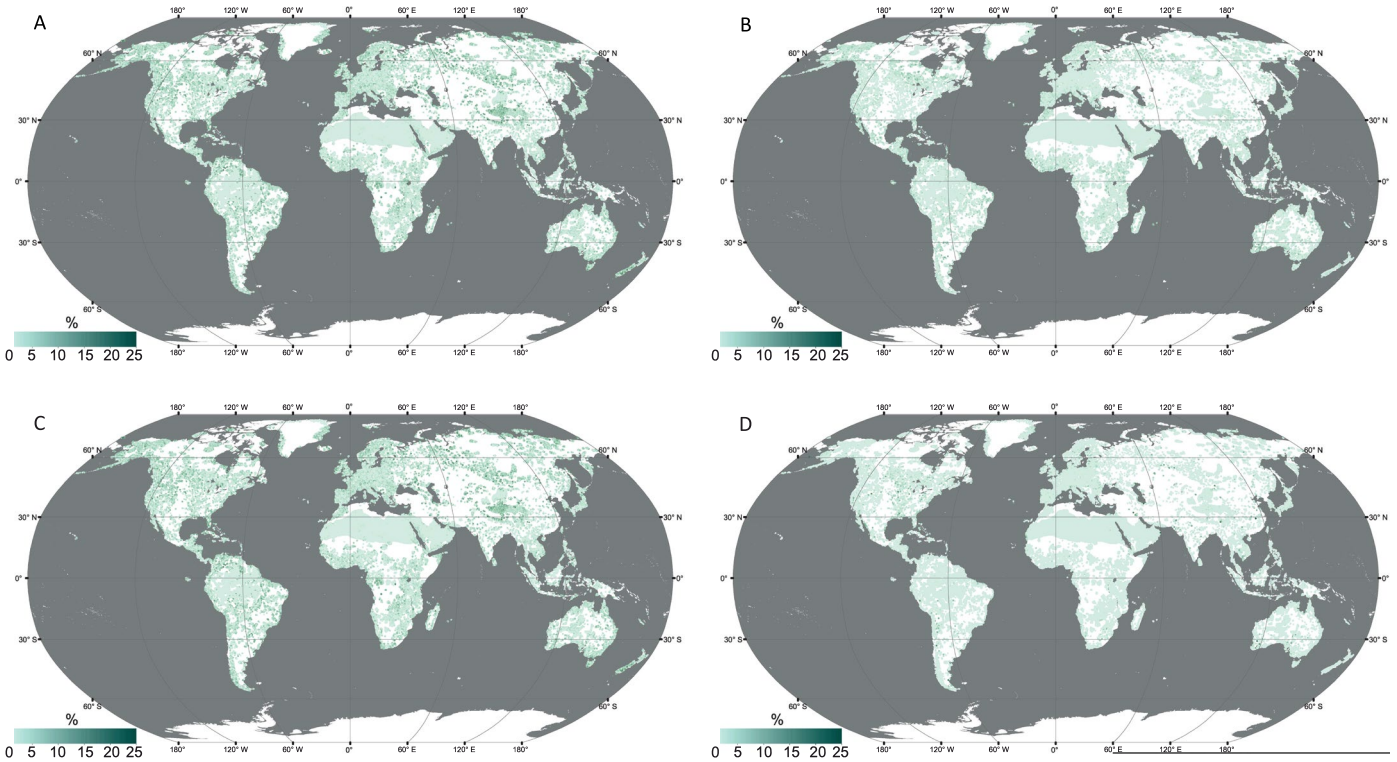

Extended Data Fig. 8 | Spatial distribution of the uncertainty of forest (A), shrubland (B), grassland (C) and wetland (D) models. Uncertainty was assessed using the standard deviation of the predictions calculated from the five sub-models originated from the 5-fold cross-validation. Uncertainty was rather low and uniform globally for all four models.

https://doi.org/10.1038/s41561-025-01742-z

Specific ecosystem type	Mean ± SD (min, max, median) (t C ha^{-1} yr^{-1})	N	Stock (t C ha^{-1})	Build-up (yr)
Boreal wetland[79]	**0.46** ± 0.57 (0.02, 2.80, 0.24)	47	373.3	811.5
Temperate wetland[79]	**2.14** ± 1.49 (0.15, 6.5, 1.65)	29	211.0	98.6
Tropical/subtropical wetland[81–90]	**1.92** ± 1.58 (0.48, 4.8, 1.32)	6	740.1	385.5
Boreal forest[78,79, 91–95]	**1.26** ± 0.11 (1.13, 1.40, 1.27)	6	129.6	102.9
Temperate forest[78,79,96–99]	**1.98** ± 0.57 (1.24, 2.80, 2.04)	7	137.9	69,6
Tropical/subtropical dry forest[78,100–109]	**1.92** ± 0.85 (0.78, 3.12, 2.11)	8	209.9	109.3
Tropical/subtropical moist forest (excl. mangroves)[78,110-121]	**3.40** ± 1.50 (1.18, 6.03, 3.64)	20	253.4	72.5
Mangrove forest/shrubland[122–127]	**1.79** ± 0.27 (1.34, 2.11, 1.72)	6	553.9	309.4
Temperate/boreal shrubland[79,128–134]	**0.59** ± 0.36 (0.21, 1.20, 0.53)	6	98.2	166.4
Tropical/subtropical shrubland[18,100–103, 135–139]	**0.31** ± 0.21 (0.14, 0.65, 0.21)	5	139.7	450.6
Temperate/boreal grassland[79,140–145]	**0.49** ± 0.16 (0.24, 0.66, 0.54)	6	79.9	163.1
Tropical/subtropical grassland[104,137,146–154]	**0.31** ± 0.21 (0.11, 0.67, 0.27)	6	68.8	221.9

Extended Data Fig. 9 | Carbon sequestration rates and carbon stocks of biome-specific ecosystem types compiled and averaged from published studies. Build-up time is the time in year required to reach the stock considering the listed rates and assuming linear trend. Data from refs. 80–153.